



Published: August 31, 2023

Citation: Williams RK, 2023. The Emerging Role of Photobiomodulation in COVID-19 Therapy – Part I: Deep-Tissue PBM Modality and Regimen for Treating SARS-CoV-2 Infections, Medical Research Archives, [online] 11(8). <https://doi.org/10.18103/mra.v11i8.4029>

Copyright: © 2023 European Society of Medicine. This is an open-access article distributed under the terms of the Creative Commons Attribution License, which permits unrestricted use, distribution, and reproduction in any medium, provided the original author and source are credited.

DOI
<https://doi.org/10.18103/mra.v11i8.4029>

ISSN: 2375-1924

RESEARCH ARTICLE

The Emerging Role of Photobiomodulation in COVID-19 Therapy – Part I: Deep-Tissue PBM Modality and Regimen for Treating SARS-CoV-2 Infections

Richard K Williams

Applied BioPhotonics, Ltd

Email: richardwilliams@appliedbiophotonics.com

ABSTRACT

Background. Infectivity, genomic variability, and symptomatic diversity of the SARS-CoV-2 virus represents a persistent challenge in the treatment of acute and long COVID-19 diseases. A direct consequence of pervasive ACE-2 receptors susceptible to the virion's spike protein, disease trajectories commence as upper respiratory infection migrating into bronchia (presenting coughing, dyspnea, and fever), followed by viremic infection and circulatory distress from inflammation of visceral epithelium and vascular endothelia, decreased blood perfusion, and hypoxia. Severe cases include hyperinflammation, cytokine storms, and multisystem inflammatory syndrome with lung and nerve damage, and chronic cognitive deficits.

Method. This paper (Part I) considers the requirements for treating acute and chronic COVID-19 with deep-tissue photobiomodulation (PBM) of sinuses, lungs and other ACE-2 populated organs using transdermal and transcranial light as a primary therapeutic modality.

Analysis. A detailed analysis of optics, biophysics, numerical simulations, and quantum photochemistry for non-invasive deep tissue PBM of SARS-CoV-2 infected organs was performed including optical design, photonic control, irradiance, fluence, modulation, and protocols.

Results. Analysis confirms 3D bendable LED pads deliver uniform light fluences into deep tissue and organs compatible with transdermal PBM treatment of whole-organ infections of the lungs, sinuses, abdominal cavity; and with transcranial PBM of neurological long-COVID. Robotic laser scanning represents another viable option for deep-tissue PBM provided the optical angle of incidence is minimal. Penetration depth depends on wavelength (not optical power) with red (635nm) and NIR (850nm) shown to adequately penetrate through cutaneous tissue and parietal fascia into viscera.

Conclusions. Red and NIR LEDs with average pulsed irradiances of 8.5 and 13.5 mW/cm² respectively deliver hands-free whole-organ deep-tissue doses of between 0.5 to 4.0 J/cm² in 60 min sessions from a surface dose of $P_{\lambda}/A = 40 \text{ J/cm}^2$ depending on tissue transmission coefficients Ψ_x at depth $x > 6\text{mm}$. The designed photonic PBM system performs algorithmic variable frequency pulsed protocols covering up to 1,200 cm². Duty factor control limits skin temperatures below 43°C irrespective of pulse modulating frequency. A mechanistic model for deep-tissue PBM, phenomenologically consistent with biophysics, photon penetration studies, COVID disease trajectories, and patient recovery profiles is presented. Part II details various acute and chronic case studies and positive outcomes thereof confirming PBM as a efficacious modality for COVID-19.

Keywords: photobiomodulation, COVID-19, long COVID, deep-tissue, penetration depth, photon energy, red/NIR wavelength, quantum photochemistry, pulse modulation, fluence model

The COVID-19 Pandemic & Beyond Epidemiology

COVID-19, an acronym for corona viral disease 2019, represents the first truly global pandemic to occur in over a century. Not since the H1N1 bird flu of 1918¹ has a disease so profoundly affected public health, global commerce, and life expectancy^{2,3,4,5}. First reported in 2020 as a severe respiratory infection of unknown origin, the discovery confounded health officials as to the cause, mode of transmission, incubation time, and infectivity. Research commenced apace to isolate and identify the pathogen.

Genetic sequencing soon revealed the culprit as a coronavirus of taxonomy within the family *Coronaviridae*. Genetically distinct from SARS-CoV and MERS-CoV viral genomes (the viruses responsible for severe acute respiratory syndrome of 2003 and the Middle Eastern Respiratory Syndrome of 2012), the new virus was named SARS-CoV-2 to distinguish it over its antecedents. Although less lethal than its predecessors, human-to-human transmissibility enabled the SARS-CoV-2 virus to spread largely unchecked. Its associated disease called COVID-19, was found to be particularly lethal in patients with comorbidities (such as immunocompromised individuals) and in aged populations. Outbreaks in senior care facilities had dire consequences.

Because at the time of its emergence, no accurate tests or targeted treatments existed, only severely ill patients were admitted into hospitals. Individuals with milder symptoms of the disease were essentially left to fare for themselves, representing an untreated undiagnosed subset of the early infected population. By July 2020 when testing finally became widely available, it was too-little too-late to contain the outbreak⁶. Prompted by the looming public health crisis, in an abundance of caution world governments decided to invoke draconian short-term travel bans, lockdowns, and quarantines in a lath ditch effort to “slow the spread”⁷.

As weeks turned into months, the commercial impact of extended shutdowns had unintended consequences – layoffs, job losses, bankruptcies, in turn precipitating a mental health crisis of job loss and personal financial stress coupled with isolation from friends and family. Cases ranged from depression and substance abuse to anxiety disorders and suicide^{8,9}. Through school closures, lockdowns caused emotional and learning deficits in adolescents¹⁰. Health care availability also suffered. Short staffed, hospitals were forced to focus on COVID care at the exclusion of other services while small private clinics,

unable to adequately manage infection risks, remained shuttered. The pandemic’s long-term impact on public health caused by postponing elective surgeries, checkups, and priority medical procedures (such as cancer therapy)^{11, 12} is not known.

Despite all these actions, the first global wave of COVID-19 was quite deadly, disproportionately targeting seniors in care facilities and those with preexisting medical conditions. Viral variants soon emerged further complicating the challenge of sustaining the efficacy of COVID vaccines and therapeutics. Because of varied global reporting and testing standards, a truly accurate assessment of the virulence and lethality of COVID-19 may never be known. For example, during the early pandemic, the number of COVID-19 cases and deaths were likely underreported, wrongly attributed to influenza and seasonal illness. After adopting widespread testing, mortality *from* COVID-19 became conflated by test statistics, i.e. unrelated deaths of patients with COVID were recorded as deaths resulting from COVID.

To best estimates, according to the World Health Organization¹³ as of February 2023 a total of nearly 750 million cases of COVID-19 have been confirmed with the death toll approaching 7 million, or approximately 0.9% mortality rate. Accounting for unreported deaths, other estimates¹⁴ place the cumulative deaths of COVID-19 at 18 million with a mortality rate of 2.4%. Despite the tragedy of COVID-19, the bird flu pandemic of 1918 was worse with over 500 million people infected and 50 million dead (a 10% mortality rate).

As we now enter COVID’s fourth year, discussions turn toward transitioning from a pandemic into an endemic phase¹⁵. And while the acute COVID-19 case load subsides, the new challenge of “long COVID” (the residual effects of SARS-CoV-2 infections) has emerged. The diverse presentations of long COVID are especially problematic for conventional pharmacology as the disease affects multiple organs and physiological systems in disparate ways¹⁶. A growing number of physicians have turned to photobiomodulation as an adjunct to post COVID standard care as the therapeutic mechanisms of light are not limited to specific organs or viral phenotypes.

Viral Phylogenetics

Coronaviruses are enveloped positive-stranded RNA viral pathogens able to cross among animal species, seven of which are known to infect humans. Three coronaviruses, specifically SARS-CoV-1 (also as SARS-CoV), MERS-CoV, and SARS-

CoV-2 (with corresponding diseases SARS, MERS, and COVID-19) are capable of causing severe illness and death in humans. Genetic and epidemiologic investigations indicate most human coronaviral infections to be zoonotic in origin. SARS-CoV-1 spilled over from masked palm civets infected by bats¹⁷. MERS-CoV passed from bats to camels to humans¹⁸. The origin of SARS-CoV-2 is less certain^{19,20}.

Although, the SARS-CoV-2 virus sequence is 96% identical to the bat coronavirus RaTG13, to date, no natural animal reservoirs of SARS-CoV-2 have been found in the wild²¹. RNA sequencing suggests the pathogen comprises a new genomic sequence of unknown origin hypothetically a recombinant of a bat coronavirus emerging in an unknown intermediate host²². Regardless of its genetic origins, what is known is the virus is transmissible from animal-to-human (zoonosis), from human-to-animal (reverse zoonosis)²³, and from human-to-human (contagion). Direct human transmission distinguishes SARS-CoV-2 from other coronaviruses.

Curiously transspecies transmission of SARS-CoV-2 is species dependent, with some mammals (tigers, lions, minks and ferrets) significantly more susceptible to infection than others. Studies reveal COVID-19 susceptibility is associated with mammals expressing a preponderance of ACE-2 receptors in both the upper and lower respiratory tract. Animals lacking the receptor (such as most livestock) are unlikely to be infected or to serve as intermediate hosts for coronavirus infection or evolution^{24,25}. The ACE-2 receptor is also recognized for its significant role in person-to-person transmission as the primary attachment point for the virion's spike protein. As such, the distribution of ACE-2 receptors by tissue type is useful for correlating disease symptoms to the organs affected, and insightful in designing pharmacological and photobiomodulation therapeutic strategies^{26,27}.

The dominant mode of SAR-CoV-2 transmission is inhalation of room air carrying fine droplets and aerosol particles containing the infectious virus²⁸. This form of exposure is most pronounced in close proximity to infected persons actively shedding the virus (i.e. within 2 meters). Aerosol transmission can also occur in enclosed spaces with inadequate ventilation, especially in densely-populated rooms and for extended duration exposures (over 15 minutes). Larger droplets, too heavy to float in the air for extended periods, may still be spread by coughing or sneezing (so called splashes and sprays). If inhaled, these viral laden droplets attach to mucosal airway

epithelial cells (AEC) of the sinuses. Yet another mode of transmission involves contacting infected tissue or surfaces then transferring the virus to the nose, face, or eyes. This indirect transmission is less prevalent on surfaces exposed to sunlight, where ultraviolet light (especially UV-C) rapidly degrades the virus, interfering with its ability to invade a host cell or to replicate. Violet (403 nm) light is also found to degrade the viability of the virus. Neither UV or violet light, however, are able to penetrate into deep tissue and therefore are not candidates for PBM modalities.

COVID-19 Pathophysiology

Viral Entry. Coronavirus infection of a host occurs via a viral spike protein contacting a target host cell membrane. In the case of SARS-CoV-2, viral entry involves two component spike proteins – subunit S1 responsible for bonding to a suitable receptor, and subunit S2 facilitating pore formation and viral fusion with the cell membrane, a biochemical reaction catalyzed by the endogenous protease TMPRSS2 aka transmembrane protease serine 2²⁹. The process of viral attachment is not a “targeted” attack *persé*, but involves a high-affinity interaction between structurally complementary receptors present on the viral capsid's S1 spike protein and on the host cell membrane. Attachment affinity is not precisely deterministic, but statistical, with some conforming matches more likely to result in viral entry and cellular infection than others. One such receptor particularly susceptible to SARS-CoV-2 attachment is the ACE-2 protein.

Present in both membrane and circulating soluble forms, the catalytic proteins mACE-2 and sACE-2 are highly ubiquitous, located throughout organs and vascularization in humans and other mammalian species. An acronym for angiotensin-converting enzyme 2, ACE-2 is a zinc metalloenzyme and carboxypeptidase. ACE-2 functions as a integral component of the renin-angiotensin-aldosterone system (RAAS) facilitating homeostatic regulation of blood pressure^{30,31}. Circulating soluble ACE-2 lowers blood pressure by catalyzing the hydrolysis of angiotensin II (a vasoconstrictor peptide) into angiotensin (a vasodilator) by attaching to MasR, a G protein-coupled receptor (GPCR) present in endothelium, locally regulating vasodilation³². ACE-1 is the antagonist for ACE-2 responsible for vasoconstriction, counterbalancing the vasodilative effects of ACE-2 activation.

Countless studies confirm the role of ACE-2 as the predominant (but not exclusive) viral entry site for both SARS-CoV-1 and SARS-CoV-2 infections in humans^{33,34,35,36}. Located throughout

the body and across different physiological systems, the broad distribution of ACE-2 receptors bestows upon SARS-CoV-2 its unfortunate ability to infect (and affect) multiple organs, thereby enabling COVID-19 to manifest a wide range of disparate clinical presentations.

Aside from serving as a viral entry site, attachment of the spike protein to the ACE-2 receptor deactivates its role in vasodilation. Specifically, upon binding to SARS-CoV-2 spike protein, the decreased catalytic activity of ACE-2 receptors. Since the virus does not affect the ACE-1 receptors, the presence of spike proteins imbalances the ACE-1 / ACE-2 ratio reducing the steady-state conversion rate of angiotensin II to angiotensin³⁷. A higher angiotensin II supply in turn promotes a net increase in vasoconstriction impeding blood perfusion and increasing localized blood pressure – conditions all classically symptomatic of circulatory dysfunction. Somewhat expectedly, lower concentrations of circulating soluble sACE-2 are correlated with COVID-19 disease severity and may hold promise as a potential biomarker thereof³⁸.

ACE-2 is not the only host vulnerability to SARS-CoV-2 viral entry³⁹. Other molecular targets include CD147, a transmembrane glycoprotein expressed in the brain and kidney. Present in inflamed tissue and in tumors, CD147 is implicated in enhancing comorbid susceptibilities. Neuropilin (NRP), a regulator of the vascular endothelial growth factor (VEGF) controls angiogenesis and vascular remodeling. NRP is expressed in the GI tract, lung, prostate, ovaries, and in endothelial cells, excitatory neurons, and olfactory epithelium of the nasal cavity. Overexpression of VEGF can lead to inflammation and edema, making NRP a likely suspect for early phase SAR-CoV-2 infection in the AEC of the upper respiratory tract.

Dipeptidyl peptidase 4 (DPP4 aka CD26) an immune system related ectopeptidase (previously identified in MERS-CoV infections) has recently been implicated by SARS-CoV-2 spike S-protein binding studies as an entry candidate. DPP4 is broadly expressed in kidneys, lungs, smooth muscle, liver and capillaries. Another suspect newly under investigation for viral entry is alanyl aminopeptidase (ANPEP). Structurally similar to ACE-2, ANPEP is highly expressed in the ileum, colon, rectum, liver, kidneys, skin, and in the conjunctiva. Viral entry in ocular membranes by ANPEP, ACE-2, TMPRSS2, and the extracellular matrix metalloproteinase inducer EMMPRIN (aka basigin or BSG) presents severe COVID-19 infection risk to the eyes^{40, 41, 42}.

Incubation. SARS-CoV-2 comprises a positive-sense single strand RNA virus. After entry, the virus sequesters the host's organelles and commences translating its viral RNA genome into structural and accessory proteins. The RNA is then replicated to form new virions released to infect neighboring host cells⁴³. The genome of SARS-CoV-2 is one of the largest among known RNA viruses, comprising of at least 26 identified protein-coding loci⁴⁴. Positive-sense RNA viruses like SARS-CoV-2 were previously thought to encode proteins solely on the positive strand. Recently however it was demonstrated negative-sense viral RNA strand intermediates arising during replication of its positive-sense RNA source-code also manifest protein-coding potential. In the case of SARS-CoV-2, *nine* new negative-sense open reading factors (nsORFs) have been identified. The function of dual-direction protein encoding and its impact on COVID-19 infectivity is unknown at this time but may increase transmissibility through enhanced viral amplification.

The incubation period for COVID-19, the time between exposure to SARS-CoV-2 and when the first symptoms appear, is estimated to range between 2-to-14 days with an average of 5 days. 97% of the symptomatic population shows signs of infection within 11.5 days^{45, 46}. According to published reports, between 32%-to-40% of the SARS-CoV-2 infected population is asymptomatic for COVID-19 conditions^{47, 48} with variability demonstrated across viral variants. Although studies suggest asymptomatic and presymptomatic persons exhibit lower viral loads, reduced viral shedding, and reduced infectivity⁴⁹, more studies are required to quantify exposure risks especially as each new variant with unique phenotypes emerge.

Disease Trajectories. As with any infection, severity depends on an individual's health condition at the time of exposure and on the pathogenicity of the contagion. The pathogenesis of SARS-CoV-2 infection in humans is illustrated in **Figure 1** for various exemplary disease trajectories⁵⁰. In case A, the infection is asymptomatic (or nearly so). Case B represents mild cold-like conditions (rhinorrhea, sore throat, malaise) resolving in 1-to-3 days with no residual effects⁵¹. The patient of case C experiences conditions of moderate severity including fever, muscle aches, headaches, sinusitis, intermittent coughing, and chronic fatigue – symptoms ultimately subsiding in a week or two with outcomes of no long-term adverse effects.

Case D represents a moderate-to-severe COVID-19 infection presenting fever, muscle cramps, dyspnea, paroxysmal coughing, reduced blood perfusion and hypoxia with the potential for

anosmia (loss of smell); ageusia (loss of taste); ocular inflammation (uveitis, conjunctivitis, blepharitis); mild cognitive impairment; and short-term memory loss (transient global amnesia). Without prompt and efficacious therapeutic intervention lung damage, cardiovascular injury, thrombosis, pericarditis, and myocarditis may result. Chronic conditions may include acute respiratory distress syndrome (ARDS), cardio obstructive pulmonary disorder (COPD), and required oxygen

supplementation. Case E represents a fatal COVID-19 trajectory, involving urgent hospitalization, tracheal intubation, mechanical ventilation, and runaway cytokine and chemokine storms, followed by an irreversible cascade of organ failures. The severity of immune response to SARS-CoV-2 infection is principally linked to various patient comorbidities including diabetes, asthma, obesity, cardiovascular conditions (such as hypertension), and immunodepression⁵².

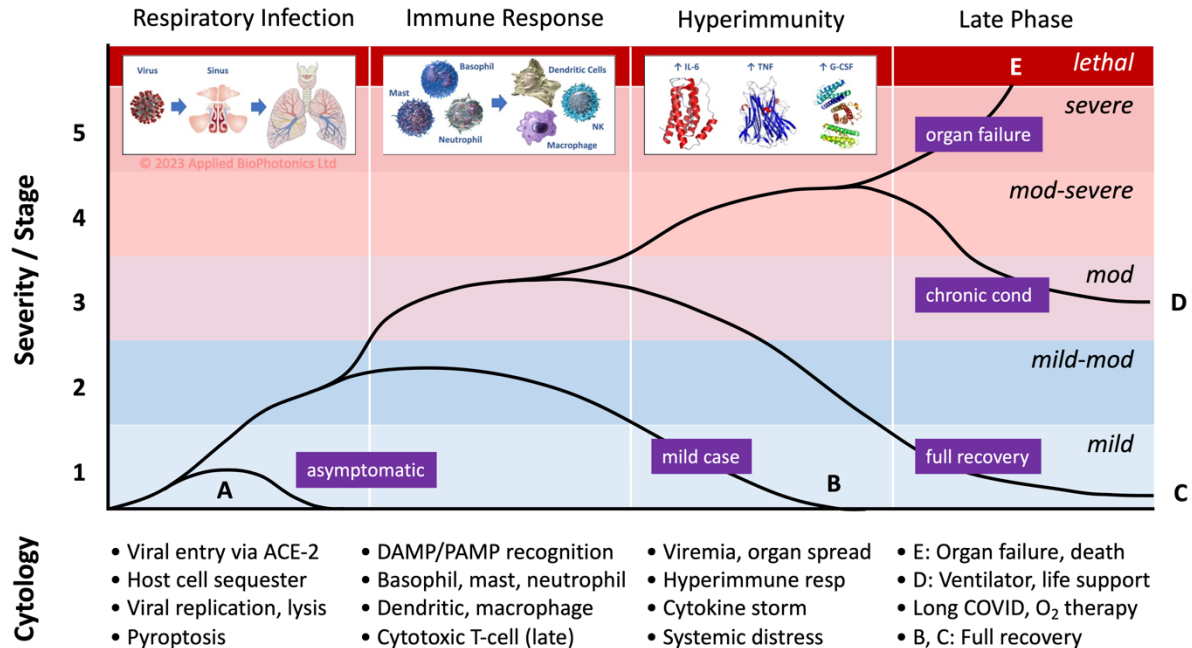


Figure 1. Various reported disease trajectories for human COVID-19 infections progressing through the phases of respiratory infection, immune response, hyperimmune response, and various late-phase outcomes including full recovery, chronic respiratory distress, and lethal organ-failure scenarios. Attribution: cellular, molecular, and organ images courtesy of Wikimedia Commons.

As depicted, the COVID infective phase involves viral entry and incubation – the interval from when SARS-CoV-2 penetrates a host cell, replicates itself, then breaks out to infect new cells (lysis), sequestering increasing numbers of host cells (viral amplification). During human transmission, aerosols containing SARS-CoV-2 enter the nasal and pharyngeal epithelia injecting viral genomic components into airway epithelial cell (AEC) cytoplasm for multiplication. The viral replicants are then released into the esophagus and trachea, ultimately invading bronchia of the lungs. Meanwhile, the original host AEC dies scattering cellular debris further promoting local inflammation and tissue necrosis (pyroptosis). Concurrently, spike protein bound ACE-2 receptors cause edema, vasoconstriction, and inflammation, potentially prompting thrombosis and fibrosis.

Photobiomodulation during the incubation phase interferes with viral replication preventing amplification, offering the potential of prophylaxis even after direct exposure to infectious spreaders.

Immunopathology. In the second phase, normal immune response is activated through recognition of pathogen-associated molecular patterns (PAMPs) by toll-like receptors (TLRs) and by mast cells sensing damage-associated molecular patterns (DAMPs). While these molecular watchdogs favorably support host-cell defense, they potentially risk a pathological inflammatory response (i.e. overreaction) implicated in hyperimmunity and autoimmune diseases. Notably, immunoresponse is a progressive process where early cytological responders comprising mast cells, phagocytes, basophils, and eosinophils, followed by recruitment of neutrophils collectively promote

wound healing in visceral epithelium and vascular endothelium.

Unfortunately, if viral replication proceeds undeterred the immunoresponse necessitates stronger cytotoxic agents to finish the job. These cytotoxic immune cells, including macrophages, dendritic cells, natural killer (NK) cells, along with adaptive T-cell and B-cell lymphocytes, release and up-regulate cytokines, powerful anti-infective pro-inflammatory enzymatic proteins designed to destroy pathogens at all cost (even at the expense of damaging host tissue).

Cytokines comprise a diverse spectrum of agents that include interleukins (IL-6, IL-2, IL-10, IL-12); interferons such as IFN- γ (interferon-gamma) and IP-10 (aka CXCL10, an acronym for CXC-motif-chemokine-ligand-10); G-CSF (granulocyte colony-stimulating-factor-3); and tumor necrosis factor (TNF). Other cytokines involved in platelet activation, endothelial dysfunction, and thrombosis include MCP-1 (monocyte chemoattractant protein-1) and MIP1 α (macrophage inflammatory protein 1-alpha). Along with IP-10, these cytokines are considered a valuable inflammatory biomarker for monitoring COVID-19 severity⁵³. Key inflammatory biomarkers correlated to COVID-19 mortality include serum C-reactive protein (CRP), lactate dehydrogenase (LDH), and ferritin⁵⁴. Other markers include neutrophil and lymphocyte counts; neutrophil/lymphocyte ratio (NLR); fibrinogen; and D-dimer levels⁵⁵; along with albumin and erythrocyte sedimentation rate⁵⁶. Multivariate analysis of low-grade inflammation or LGI (defined as CRP >0.3 and <1.0 mg/dL) in long COVID cases suggests neutrophil count, NLR, fibrinogen, and CRP show the greatest sensitivity in tracking LGI.

If cytokine and chemokine fail-safes cannot contain the infection, an increasing viral load in the sinuses and lungs will invariably *break out* to other organs⁵⁷, primarily through blood circulation (viremia). As the coronavirus spreads throughout the body, systemic inflammatory distress (a cytokine storm) then ensues^{58, 59, 60}. The prognosis for patients experiencing a COVID-19 cytokine storm involves three possible outcomes, either (i) the hyperinflammatory condition subsides and the patient fully recovers, (ii) acute symptoms subside but organ damage creates a chronic health condition (long COVID)⁶¹, or (iii) organ failure and death. PBM delivered during this phase can arrest and limit viremic spread while limiting hyperinflammatory reactions.

Therapeutic Indications

Treatment of acute and long COVID-19 today primarily involve three strategies, namely

vaccination, pharmacology and photobiomodulation. These modalities (made in accordance with medical standards of care) are not mutually exclusive and are often applied adjunctively. Each approach offers unique benefits with equally unique challenges.

Vaccines. Although vaccines are routinely used to combat infectious disease, inoculation against viruses with high genetic-variability face a constant challenge of waning effectiveness^{62, 63}. As a virus mutates, immune cells trained to detect a specific viral phenotype are no longer able to recognize the evolving molecular signature of viral proteins. Unfortunately, mutations of single-strand RNA virus such as coronaviruses are not only probable, but inevitable, as evidenced by the ongoing emergence of COVID-19 variants including the Alpha, Delta, and Omicron strains⁶⁴.

Moreover, genomic changes have been detected on the codon defining the spike protein⁶⁵, a key component used in many vaccine strategies. As the virus evolves, so too must the vaccine designed to mimic it. Although a useful tool in mitigating COVID-19 severity, inoculation has been shown to be unable to completely prevent infection and transmission, prompting renewed efforts in therapeutic stratagems. Moreover, while inoculation can minimize acute COVID-19 symptoms (indirectly mitigating long COVID severity), vaccines cannot anticipate or avoid the myriad of resulting chronic conditions, nor address associated mental health conditions therefrom.

Pharmacology. Drug interventions face different challenges. Because of the hyperinflammatory character of COVID-19, pharmacological regimens require carefully balancing anti-infective action against an overly aggressive immune response provoking a cytokine storm. Primary care and outpatient pharmacological interventions include analgesics, antipyretics, antivirals, monoclonal antibodies, and inhaled corticosteroids⁶⁶. The principal goal of such ambulatory care is to suppress viral proliferation, prevent progression into severe disease; limit respiratory distress; reduce the risk of organ damage and long COVID; and avoid the need for hospitalization and mechanical ventilation.

When early medical interventions fail to arrest severe symptoms (presenting lung and vascular inflammation, edema, viremia, and organ dysfunction), hospitalization, oxygen supplementation, and the urgent application of more aggressive therapeutic regimens become necessary. ICU pharmacology generally involves the combined application of anti-inflammatories (such as dexamethasone), antivirals (e.g. remdesivir),

kinase inhibitors, immunomodulators, and monoclonal antibodies. If SpO₂ levels continue to decline, mechanical ventilation is unavoidable.

Another challenge in treating COVID-19 pharmacologically is its broad range of extrapulmonary organ involvement. Autopsies^{67, 68} reveal SARS-CoV-2 has been found to infect at least seventy-nine tissue and organ locations, including the heart, kidneys, liver, muscles, nerves, reproductive organs, and eyes. Since infected organ and tissue types (each with their own unique biochemistry) present different symptoms of COVID-19 disease, no single pharmacological agent (or cocktail of multiple drugs) can be expected to counter the full spectrum of COVID-19 pathogenicity. Organ damage and persistent inflammation associated with long COVID presents cardiovascular disease and myocarditis⁶⁹; autoimmunity; gut microbial dysbiosis⁷⁰; cognitive dysfunction and memory loss; and diabetes. Pharmacological therapies can symptomatically treat long COVID but not prevent it. No medicines are indicated for addressing neurological deficits and mental health impacts of long COVID such as chronic inflammatory pain (neuritis), sleep disorders, persistent malaise, and brain fog.

Photobiomodulation. A third modality emerging in SARS-CoV-2 infection management and the treatment of COVID-19 disease is photobiomodulation (aka PBM). Unlike the protein-specificity of adaptive immunity conferred by vaccines (i.e. viral adjuvants to stimulate antigenic activity), or the biochemically selective mechanisms of medicines and monoclonals, PBM employs quantum photobiochemistry of energy absorption, specifically non-ionizing electromagnetic radiation (light) to modulate the cytological and molecular biochemistry of virtually all tissue types and organs in humans and mammals (and for that matter virtually any eukaryotic organism or species). Mediated through transmembrane proteins⁷¹ (e.g. Ca²⁺ ion channels, TRPs⁷², and mitochondrial cytochrome-c⁷³), the therapeutic mechanisms of photobiomodulation (PBM) are largely unaffected by biochemical disguises or mutations of viruses, bacteria, fungi, or protea intended to thwart immune response, especially those involving innate immune system reactions.

As such, the directed application of specific wavelengths of light energy impedes pathogenic reproduction of SARS-CoV-2 either by directly damaging the pathogen's structural integrity with excess energy⁷⁴ or by modulating innate immune response through reactive oxide species^{75, 76} and inflammatory pathways^{77, 78, 79}, neither mechanism of which is sensitive to viral genomic variability (i.e.

mutations). In simple terms, physics controls chemistry, not the converse. Furthermore, PBM may be used for COVID-19 disease as a primary therapeutic modality⁸⁰ or adjunctively in concert with pharmacology⁸¹. Transcranial PBM, extensively studied in the treatment of neurological disease⁸² (such as Alzheimer's-dementia (AD) and stroke) also holds promise in ameliorating the effects of long COVID on neurological conditions⁸³ (brain fog) and mental health.

Deep Tissue Photobiomodulation PBM Overview

Photobiomodulation (PBM), the photochemical effect of light on the metabolism of living cells is an incredibly complex and diverse topic⁸⁴. With hundreds-of-thousands of published papers from over 40 countries and over two million google search results, PBM topics span nearly every aspect of human and animal physiology and medicine. Photobiomodulation (PBM) involves photon absorption of light-sensitive molecules called chromophores present within cells (often comprising transmembrane proteins) influencing cellular metabolism, respiration, apoptosis, protein synthesis, and cellular defense. As a subcategory of the broader field of light therapy (or phototherapy), PBM occurs in nearly all cell types, not only in optical receptors. Topically, PBM generally excludes laser surgery and ablative procedures (e.g. intense pulse light, aka IPL).

A Brief History of PBM. While the health benefits of light have been recorded since early civilization, the scientific application of light in the treatment of disease began early in the last century, heralded by empirical medical studies by Niels Ryberg Finsen earning him the 1903 Nobel Prize⁸⁵ "in recognition of his contribution to the treatment of diseases, especially lupus vulgaris, with concentrated light radiation, whereby he has opened a new avenue for medical science." Just two years later, Albert Einstein published four papers⁸⁶ in the journal *Annalen der Physik* (the so-called *annus mirabilis* papers) one of which described interactions between light and matter (the photoelectric effect⁸⁷), forming the basis of quantum mechanics, quantum physics, and quantum chemistry, and ultimately earning him the Nobel Prize in Physics⁸⁸.

Profoundly, the paper asserted (i) light travels in discrete packets of energy called quanta (photons); that (ii) unlike matter, energy carried by photons doesn't depend on their speed but instead is proportional to the light's frequency or inversely proportional to wavelength (referred to as the Planck-Einstein relation); and that (iii) a photon must

possess some minimum in energy, an amount called the work function (a measure of bonding energy) to induce an electron energy-state transition causing action (a photoelectric effect or photochemical reaction). Molecular light absorption insufficient to overcome this work function causes only vibrational kinetic energy, manifested as heat. Together with material density and molecular structure, quantum and thermal energy absorption determines the optical and photochemical properties of solids⁸⁹. Optical absorption forms the foundational biophysics governing photobiomodulation and is critical in understanding, designing, and developing biophotonic PBM systems.

It wasn't until the discovery of the laser in 1960⁹⁰, and the subsequent developments of the semiconductor laser diode (LD)⁹¹ and the light emitting diode (LED)^{92,93} two years thereafter that the medical application of light became practical. Comprising compound-semiconductors engineered to emit specific wavelengths, these heterojunction diodes achieve high quantum efficiencies converting electrical energy into light with minimal heating or power loss.

It was soon discovered that low intensity laser light offered health benefits including stimulating hair growth⁹⁴ and accelerating wound healing⁹⁵. Since LEDs at the time were not sufficiently bright, most early biomedical research concentrated on using lasers, erroneously concluding that coherency was a key factor in observed benefits⁹⁶. The term low-level laser therapy or LLLT (now obsolete) was adopted to distinguish low power lasers (also called cold lasers) from higher power surgical lasers. Once however the medical use of LEDs became widely adopted, the acronym LLLT became problematic, firstly because of disagreement as to the acronym's ambiguous meaning (i.e. does L stand for laser, LED, or light?), and more significantly because "low-level" is purely subjective with no quantitative definition or consensus. LEDs can't even emit high optical powers. Photobiomodulation^{97,98} is now a more broadly accepted term.

By the 1990s, tremendous advancements in LED efficiency, brightness, cost, and large-areal coverage established LEDs as a compelling alternative to the lasers^{99,100}. Aided by support from NASA¹⁰¹, medical studies soon confirmed LED based therapy matched (or even outperformed) lasers^{102,103}, with the caveat that a LED light delivery system must be well designed to maximize energy coupling and prevent reflection. By the turn of the century, bendable pads containing arrays of hundreds of LEDs were first introduced (initially under the tradename APLightsource-2000). The LED

array resolved laser's problematic small spot size, overcoming the optical coupling issue of rigid LED panels while enabling concurrent PBM of large areas (face, back, thighs)¹⁰⁴. Mechanical breakage from repeated flexing, however, compromised use life.

Since that time, significant advancements in 3D-flexible LED pad design and ruggedness have been realized^{105,106}, coupled with advanced biophotonics and programable tissue-specific sequenced pulse modulation¹⁰⁷. Pulse modulation in modern PBM photonic systems is important in maintaining a safe skin temperature ($T_{\text{skin}} < 43^{\circ}\text{C}$), controlling the average delivered power or irradiance (specified in mW/cm^2), and setting the total dosage (delivered energy or "fluence") of a therapeutic PBM treatment (measured in J/cm^2)¹⁰⁸. In laser PBM, pulsing is further required to preventing laser diode overheating and to reduce burn risks and eye damage.

Factors in Deep Tissue PBM

Optical Delivery. Using PBM to treat COVID-19 infected *whole-organs* (such as lungs, liver, intestines, and the brain) is not a trivial matter as it relies on delivering significant amounts of energy to deep-tissue over large areas in reasonable times (without burning the skin). In transdermal photobiomodulation, photons must penetrate through cutaneous layers overcoming power losses from reflection, refraction, dispersion, and scattering in order to reach underlying tissue and organs. Transcranial PBM of the brain (used in long COVID therapy) must also overcome optical losses in bone. Factors affecting light transmission and optical losses during PBM therapy include the light wavelength λ , the distance between the light source and skin surface, the angle of incidence θ (the angle measured orthogonal to the skin), and the thicknesses of intervening tissue layers. Improperly engineered optical delivery is largely responsible for poor or inconsistent results reported in numerous published PBM studies, especially those involving LED therapy of deep tissue and scanned laser treatment of whole organs.

In deep tissue PBM, light must first travel from a light source (LED or laser) to the patient, then successfully traverse the interface between air and upper epithelial tissue before penetrating into the dermis and body cavity. Governed by Maxwell's equations for electromagnetic radiation (EMR), a simplified form of classical wave equation includes the inverse-square law for propagation in free space or air, and the laws of geometric optics at an interface¹⁰⁹, namely the law of reflection and Snell's law of refraction. Specifically, the inverse-

square law states the effective brightness of an incoherent light source (like a lamp or LED) diminishes as it disperses covering larger areas with increasing distance. As such, area normalized optical power P/A given by the relation $P/A = P/(4\pi d^2)$ means a doubling the distance d from the LED to the skin reduces surface brightness (measured in mW/cm^2) by a factor of four.

The inverse square law highlights the need for a LED light source to contact or maintain close proximity to tissue being treated. Power losses occurring at the air-to-skin interface determine what portion of impinging light penetrates the epithelium to reach deep tissue targets. While some light may pass through the skin's surface, other light beams are reflected and their energy lost. Because the atomic density of skin differs from air, the speed of light slows in proportion to the ratio of refractive indices of the transmitting mediums. This speed change causes light beams to emerge at different angles than at entry, a phenomenon called refraction. Light redirected off-angle (i.e. not perpendicular to the skin's surface) travels a longer more indirect path than when orthogonally oriented increasing the statistical probability of being absorbed in the skin without penetrating into deeper tissue targets.

Moreover, because skin is amorphous with no single crystalline direction and no uniform plane of reflection, scattered light beams cause more scattering further enhancing power loss in the upper layers of skin. Refractive and scattering power losses are higher for light impinging the skin off-axis, i.e. for larger angles of incidence θ characteristic of lamps, distant light sources, scanned laser light, or planar LED-panels illuminating curved portions of the body. For this and other reasons, rigid LED panels, wall LEDs, and LED beds (used in skin care) are less suitable for deep-tissue whole-organ PBM.

Handheld probes and wands (whether LED or laser) although offering efficient optical coupling, are problematic in treatment of infectious diseases such as COVID-19 as they require a therapist to maintain close proximity to an infected patient for extended durations. During a session the therapist must hold the light probe or wand in place (without moving) for some duration, then reposition it, repeating the entire procedure again in a new location. Even for an unusually large-area cluster probe (e.g. covering 5 cm^2) with multiple LDs, treating a lung area of 300 cm^2 requires dozens of placements. Laser probes cover smaller areas requiring even longer sessions. The longer a therapist must stay in close proximity to an infected patient, the greater the chance they will contract COVID-19.

Excluding the foregoing methods from consideration, two hands-free forms of optical delivery have been used successfully in treating COVID-19 patients – laser scanners¹¹⁰ and conformal LED pads¹¹¹. Since laser scanners employ a coherent light source with minimal dispersion, lasers do not suffer the same power loss in free air as LEDs. Able to maintain a relatively constant size and brightness within the laser spot, laser irradiance (brightness) is mostly insensitive to the distance between the laser diode light source and the patient. Unfortunately, because of a laser's intrinsically small spot dimension, beam scanning is required to treat large areas for whole-organ therapy. Laser scanning is not without its own challenges.

During laser scanning, a mechanical or robotic arm suspended above a patient contains a laser head unit that serially rasters emitted laser light across a patient's back in a predefined pattern. Serial rasterized scanning requires tens-of-minutes, during which time a patient laying in a prone position must remain perfectly still to ensure uniform illumination and dosing. Doctors report that COVID-19 patients with severe pneumonia complain of dyspnea and breathing discomfort when laying face down in a prone position.

Patient discomfort thereby is a disadvantages posterior laser scanning as a viable therapeutic option for awake patients. As an aside, it should be noted that it is a common misconception that proning improves breathing. A recent clinical trial reported by JAMA¹¹² concluded "prone positioning offered no observed clinical benefit among patients with COVID-19-associated hypoxemia who had not received mechanical ventilation. Moreover, there was substantial evidence of worsened clinical outcomes."

The alternative, anterior laser scanning of the chest and lungs, represents an uncertain eye safety risk as unattended patients isolated in a treatment room may inadvertently remove safety glasses during a session with potentially harmful effect. Eye safety around lasers is a complex subject as it must consider a number of risks including an unattended patient removing their glasses.

Another complexity of laser scanning is beam uniformity. Because scanning involves a dynamically changing angle-of-incidence θ , epithelial scattering and penetration depth vary. While perpendicular delivery exhibits less than 5% energy loss to reflection, off-axis beams lose significant energy to reflection and refraction impacting PBM dose and penetration depth, especially for angles over 40° from the vertical¹¹³.

As an alternative, deep-tissue whole-organ PBM therapy can be performed using bendable LED pads. By conforming to body contours, optical coupling of flexible LED pads can be highly efficient with minimal reflective and refractive losses. Unfortunately, consumer light pads using neoprene and porous rubbers are unsanitary, causing skin allergies, trapping microbes, and risking infectious spread. Moreover, traditional flex printed circuit boards (PCBs) used in most LED pads are wholly unsuitable in clinical settings, routinely experiencing reliability failures from repeated bending. Dominant failure modes include open-circuits from tearing of the PCB film, cracking of conductive

traces, and breakage of LED solder joints causing dead LEDs across the pad.

To overcome these deficiencies, a new generation of LED pad was developed comprising high-temperature aseptic hypoallergenic polymer pad covers combined with a special hybrid PCB design of heterogenous construction containing redundant interconnects ¹⁰⁵. Redundant circuitry means interconnection failures do not cause a corresponding electrical malfunction. Deployed commercially over the last nine years, the innovation shown in **Figure 2** is designed to reliably and repeatedly bend in 3D, maintaining uniform irradiance and depth without breaking, and to facilitate easy cleaning and disinfection.

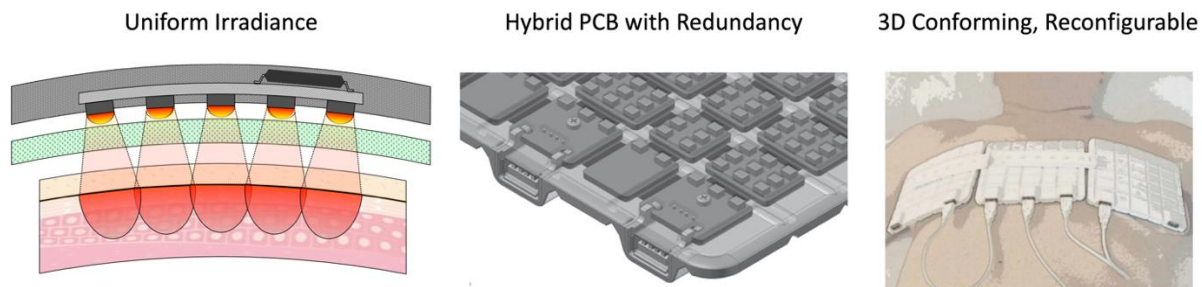


Figure 2. Optical delivery using 3D bendable LED offering uniform irradiance over large areas, hybrid PCB with redundant interconnects to mitigate breakage and open circuit failures, and body conforming aseptic polymeric pads reconfigurable for coverage areas from 200 cm² to 1,200 cm². Patents issued and pending ¹⁰⁵.

Each pad used in COVID-19 case studies (discussed in Part II of this paper) covers 200 cm² with more than 200 LEDs per pad. Able to drive six LED pads simultaneously from a single PBM controller (capable of sourcing over 18W), the pads may be reconfigured to cover any body part uniformly delivering light to internal organs including anterior or posterior lungs, sinuses, and liver-spleen-intestines (gut). A separate headband-shaped pad (not shown) is employed for transcranial (tPBM) therapy.

Deep-Tissue Photon Transmission. Since SARS-CoV-2 infects visceral organs and blood vessels, a fundamental requirement in PBM therapy of COVID-19 is deep-tissue photon transmission. Deep-tissue transdermal PBM of visceral organs requires light of longer wavelengths to travel through cutaneous and subcutaneous tissue reaching the abdominal cavity while carrying sufficient energy to elicit a photochemical (not a photothermal) response. Specifically, the Planck-Einstein relation describes a photon of wavelength λ (or frequency f) possesses energy E given by

$$E = hf = \frac{hc}{\lambda}$$

where h is Planck's constant and c is the speed of light.

Although the equation stipulates that shorter wavelength light has more energy than longer wavelengths (e.g. ultraviolet has more energy than red light), the penetration depth of higher energy photons is not necessarily deeper – behavior completely counterintuitive to Newtonian physics. Instead quantized photochemical interactions among molecules, electrons, and photons govern whether specific wavelengths are absorbed or scattered, key factors determining if light reaches deep tissue or remains relegated to the dermis. As such, light penetration depth is not based on optical power but on wavelength, modulated by light-absorbing molecules (chromophores) populating intervening tissue layers.

Quantized photochemical interactions controlling light penetration depth are mathematically problematic because the quantum electrodynamic behavior of solids (including light absorption, excitation, and relaxation) exhibit

probabilistic rather than deterministic behavior. Other complicating factors governing absorption and transmission include inhomogeneity in cutaneous strata. By simplifying quantum photochemical effects as wavelength-dependent bulk material properties (characterized by absorption and scattering), light penetration can be approximated as a non-iterative differential equation referred to as the Beer-Lambert law^{114,115}. Assuming molecular attenuators operate independently from one another (as a linear system) and the attenuating medium is homogeneous with minimal scattering (low turbidity), then the Beer-Lambert law for radiant flux (aka irradiance) $P(x)/A$ at depth x can be simplified to an exponential decay within specific layer given by

$$\frac{P(x)}{A} = \frac{P_\lambda}{A} e^{-\mu x}$$

where μ is the Napierian (i.e. base e) attenuation coefficient, and P_λ/A the irradiance at the plane of incidence penetrating the each overlying block. The equation describes an exponential decay of characteristic length $\delta = 1/\mu$ where the attenuation coefficient can be approximated in terms of absorption and scattering coefficients μ_a and μ_s by the relation

$$\mu = \sqrt{3\mu_a(\mu_a + \mu_s)}$$

representing an approximation valid for a moderate degree of scattering in a homogeneous material. The law can be restated in terms of depth

$$x = -\frac{1}{\mu} \ln \frac{P(x)}{P_\lambda}$$

where the transmitted light fraction $P(x)/P_\lambda$ is the ratio of flux density at depth x as a fraction of surface flux P_λ . When $P(x)/P_\lambda$ drops to a relative brightness of $1/e \approx 37\%$ of the surface irradiance, then $x = 1/\mu = \delta$, the characteristic length of the exponential decay.

The depth δ is often mischaracterized as *penetration depth* (the depth light travels) even though more than a third of the photon flux remains unabsorbed at this depth. A more apposite definition for penetration depth is the maximum distance in biological tissue able to meet the minimum irradiance criteria required by a particular application. Since the requisite brightness

for pulse oximeters, infrared imaging, PBM therapy, and photodynamic therapy (PDT) differ, so too does the applicable definition of optical penetration depths. PBM, for example can be efficacious at 0.5% provided surface irradiance P_λ is sufficiently bright, while activating injected nanoparticles in PDT demands a higher flux density.

Unfortunately, skin is not homogeneous in composition and scattering is more significant in the upper layers (stratum corneum, epidermis) than in deeper tissue. To more accurately depict skin for simulating photon transport, each layer should be represented as a homogeneous block with an incoming surface brightness equal to the light exiting the overlying layer, and delivering light to the surface of the block underlying it. The difference between incoming and outgoing optical flux represents power loss within each cutaneous layer. Given its complexities, quantitative analysis by numerical computer simulation is more insightful than algebraic approximations in predicting photon penetration and absorption. Precision however relies on simulation parameters.

Finlayson et al¹¹⁶ modeled skin-light interaction using Monte Carlo analysis for direct, off-angle, and diffuse light sources. The model divides the skin into six layers based on a model of Barnard et al¹¹⁷ comprising a characteristic thickness and corresponding optical properties (absorption μ_a and scattering coefficients μ_s as a function of wavelength) representing the influence of various chemical and biochemical molecules present each layer (e.g. water, melanin, oxygenated and deoxygenated hemoglobin, and lipids). Especially noteworthy is optical absorption of hemoglobin between 500-600 nm (the Q-band present in the dermis and subcutaneous layers) and another peak at 970 nm due to water absorption in all layers.

The model's stratified ordered layers of skin and corresponding thicknesses include (i) stratum corneum, 20 μm ; (ii) epidermis, 64 μm (thickest case); (iii) melanin layer, 10 μm ; (iv) basal layer, 10 μm ; (v) dermis, 2 mm; and (vi) subcutaneous tissue or hypodermis including adipose and superficial fascia, 3 mm. **Figure 3** illustrates the reported light transmission by depth from the skin's surface as a function of light wavelength (adapted from¹¹⁶). Note that for illustrative purposes the graph's ordinate (y-axis) is a composite of a linear scale for depths greater than 1 mm, and a log scale for depths below 1 mm (hence no "0" is labelled on the ordinate axis).

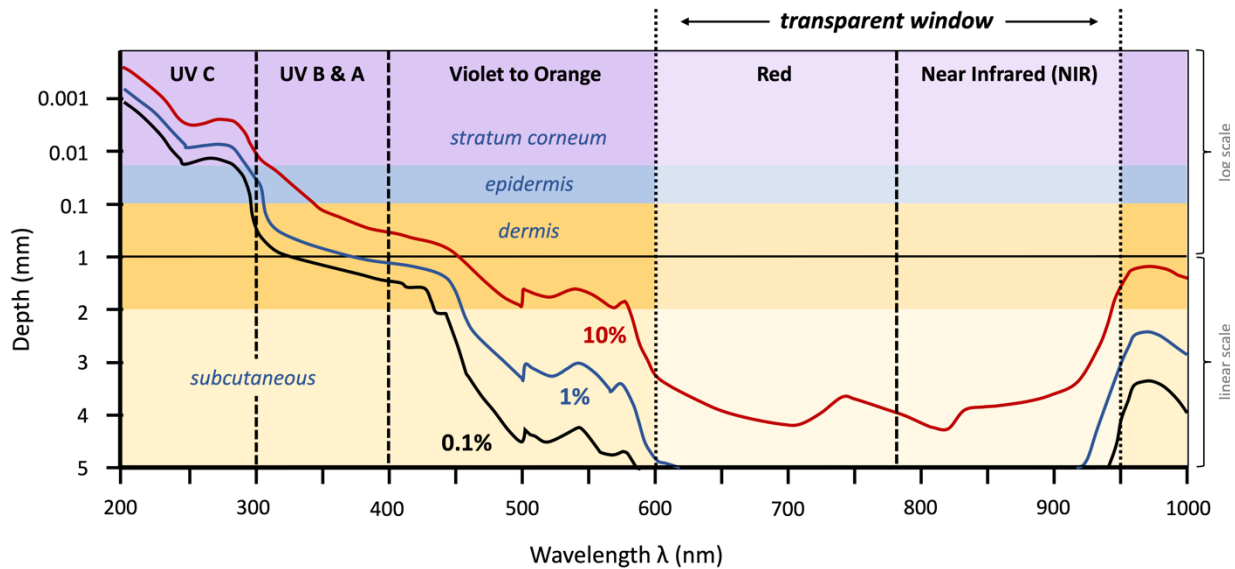


Figure 3. Monte Carlo simulation of optical penetration of ultraviolet ($\lambda < 400$ nm), visible ($400 \text{ nm} \leq \lambda < 780$ nm) and near infrared light ($780 \text{ nm} \leq \lambda$) into epidermis, dermis, and hypodermis, after Finlayson ¹¹⁶

Observations confirm the general trend that shorter wavelength light (UV, violet, blue) penetrates to shallower depths than longer-wavelength red and near infrared (NIR) radiation. Specifically, the non-ionizing portion of the electromagnetic spectrum, i.e. shorter wavelengths than red light ($\lambda \leq 600$ nm) is essentially relegated entirely to the epithelium, unable to penetrate into deep tissue or visceral organs. So, despite the demonstrated virucidal capability of ultraviolet ¹¹⁸ and violet (405 nm) light ¹¹⁹, short wave radiation cannot reach internal organs.

Although longer wavelength light penetrates more deeply, the absorption spectrum of water blocks significant optical penetration in the near infrared spectrum above 950 nm. Conversely, hemoglobin absorption of visible light below 600 nm also substantially blocks light transmission. The spectrum between 600 nm and 900 nm is generally described as the therapeutic window ¹²⁰ (aka optical window or near-infrared window) where light can penetrate into the body unobstructed by blood, water, and epithelium.

The precise range of the biological transparent window in human skin is somewhat subjective, depending on the definition of

transparency. For example, a more liberal definition of the window extends from 600-to-1300 nm ¹²¹, expanded to include a secondary local minimum in water's absorption spectra around 1060 nm ¹²². Consistent with the water absorption model, independent studies using bovine tissue samples confirm 808 nm of light penetrates as much as 54% deeper than 980 nm light ¹²³. Other studies confirm full depth penetration requires an optical source wider than 8-to-30 mm ^{124, 125} depending on wavelength, a factor adversely impacting small spot laser probes but irrelevant for 200 cm² LED pads.

Figure 4 illustrates exemplary abdominal tissue comprising 5.2 mm of epithelium overlying 1 mm parietal fascia and ~100 μm visceral fascia ¹²⁶. Based on Monte Carlo (solid) and Beer-Lambert (dashed) analysis, the graphic also depicts transdermal absorption and transmission of wavelengths in the red and NIR spectrum of the transparent optical window. While the results are insightful, reported absorption and scattering tissue properties dramatically vary ^{127, 128, 129}. Along with overly simplified models of vascularization, simulation discrepancies are pervasive, and especially problematic when predicting deep-tissue penetration below 2 mm.

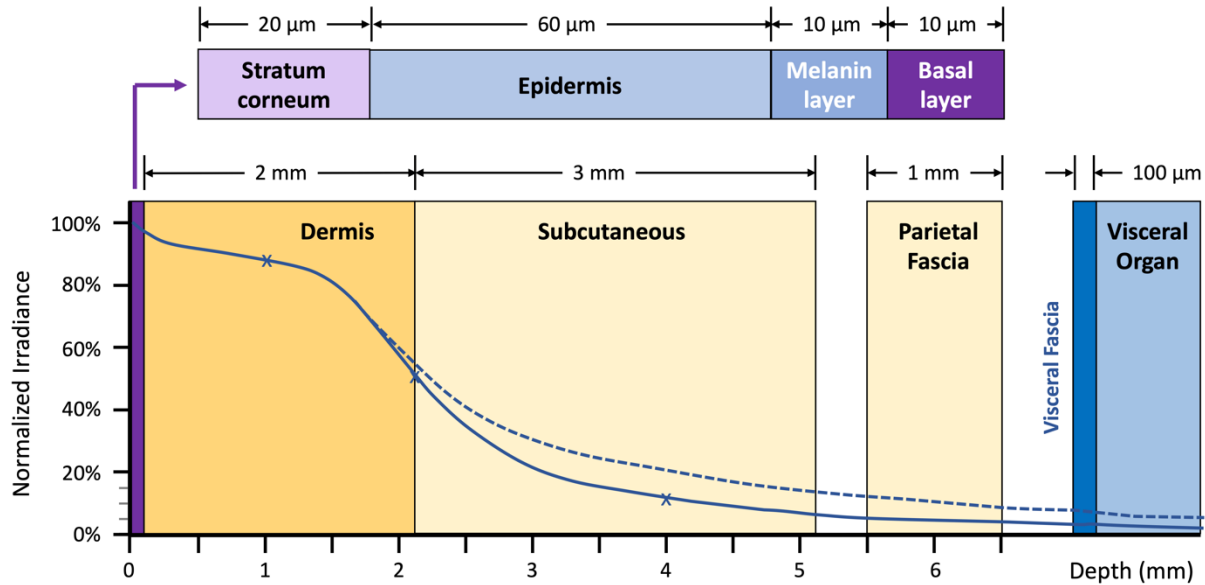


Figure 4. Transdermal transmission approximations of red and NIR light in epidermis, dermis, subcutaneous, and parietal fascia penetrating pleural and abdominal cavities and visceral organs therein. Solid line adapted from simulation ¹¹⁶, dashed line from modified Beer-Lambert analysis. For deep tissue properties, refer to ¹²⁶. Layer thicknesses optical material properties, and irradiances are exemplary and may vary by patient and organ.

Moreover, numerous competing Monte Carlo simulations papers show conflicting results ^{130, 131, 132}. In particular, because the subcutaneous layer is the thickest portion of the epithelium, minor differences in subcutaneous absorption and scattering coefficients μ_a and μ_s and variation in thickness assumptions produce disproportionate effects.

Curiously, the simulation indicates that red and NIR light penetrate to approximately the same maximum depth, a conclusion in conflict with several reported measurements showing 850 nm NIR penetrates more deeply than 635 nm red light, up to 200% that of simulations ¹³³. Optical measurements of human cadavers ¹³⁴, human cheek transmission ¹³⁵, rat skin ¹³⁶, and pork skin ^{125, 137} indicate optical penetration is deeper than what simulations suggest. Since optical penetration is a key parameter in deep-tissue transdermal therapy of the lungs, sinuses, and other ACE-2 populated organs at risk from acute and long COVID, an accurate accounting for the incongruencies between simulation and empirical measurements is warranted.

Similarly, analytical ^{138, 139}, cadaveric ¹⁴⁰, and therapeutic ^{141, 142, 143} studies likewise confirm significant transcranial transmission of red ¹⁴⁴ and NIR ¹⁴⁵ light into and throughout the brain ^{146, 147, 148} including the prefrontal cortex, the hippocampus, corpus colosum, and brain stem. Transcranial PBM

of the brain lobes is important in the treatment of neurological symptoms of long COVID.

Irradiance (Power, Brightness). Optical power delivered to the surface of the skin is referred to the irradiance of a light source. Equally applicable for a focused laser beam or a LED array in virtual contact with the skin, irradiance P_λ is defined as the optical brightness at the skin's surface (i.e. at $x = 0$) measured either in mW or scaled by area as P_λ/A (as mW/cm²). Similarly, light reaching a tissue target at depth x for PBM therapy is defined as $P_{trgt}(x)$ or $P_{trgt}(x)/A$.

The unitless optical power transmission coefficient $\Psi_{trgt}(x)$ is thereby defined herein as the ratio of optical power reaching a tissue target or organ divided by the surface power P_λ given as

$$\Psi_{trgt}(x) = \frac{P_{trgt}(x)/A}{P_\lambda/A} = \frac{P_{trgt}(x)}{P_\lambda}$$

By varying tissue thicknesses, optical absorption, and scattering parameters in combination with a literal plethora of values reported for skin and fascial layers, numerical and analytic models predict the transmission coefficient $\Psi_{trgt}(x)$ ranges from 0.7% to 7% with the best penetration into the sinus and lungs and the poorest optical coupling into the abdomen (where thick subcutaneous and visceral adipose generally accumulates with age). Penetrating light not delivered to the target tissue

is mostly lost as heat. Factors influencing deep-tissue irradiance profiles include photon emission, thermal losses, absorption, and pulsing (but not coherency or monochromaticity).

Photon Emission. During light emission, the optical power P_λ of a LD or LED is defined as its electrical input power times its efficiency, or in terms of diode current I_D and semiconductor forward junction voltage V_j by the relation $P_\lambda = \eta P_{in} = \eta(I_D \cdot V_j)$. The term η , the energy power efficiency (EPE), describes the ratio of optical watts emitted divided by the electrical power input having units of $W \cdot W^{-1}$. Normalized to area, the incident optical power (with units of mW/cm^2) becomes $P_\lambda/A = \eta V_j (I_D/A)$ where P_λ/A has units of mW/cm^2 and where I_D/A represents the diode's current density in mA/cm^2 . LED brightness and uniformity thereby depends on current, not voltage.

The value of η varies depending on the semiconductor material used, its associated fabrication technology, and the wavelength of emitted light. In general light wavelength is inversely proportional to a material property called "bandgap". Wide bandgap (WBG) materials (like SiC or GaN) require higher forward voltages and produce shorter wavelength photons (e.g. UV, blue) than narrower bandgap compounds used in red and NIR devices.

For complex reasons involving semiconductor physics and bipolar (hole and electron) carrier transport, wide bandgap materials exhibit lower quantum conversion efficiencies. Theoretically, then longer wavelength LEDs should be more efficient¹⁴⁹. That said, given the recent global focus on energy-efficiency in solid-state lighting, WBG semiconductors are rapidly advancing technologically thereby offsetting any intrinsic material disadvantages. As such, efficient LEDs ($\eta > 50\%$) are now ubiquitous, available in most colors across the EMR spectrum.

Thermal Losses. Since medical-grade PBM systems are generally not battery powered (too much energy), the value of η is not an issue of system efficiency but of self-heating. Specifically for a given optical output power, a lower η diode produces less light and more heat. Self-heating in LEDs and LDs has several disadvantages including reduced light output (sag), shorter device life, higher operating temperatures, and at excessive levels – patient burn risk. As such, continuously overdriving an LED or LD is not recommended for PBM applications.

Thermal losses occur through three elements (i) in the semiconductor light source, (ii) in photonic drive circuitry, and (iii) in tissue overlying the organ

target. Heat Q_{semi} produced within the semiconductor LED or LD device represents the fraction of electrical power that is not converted into light, expressed per device by $Q_{semi} = (1-\eta)V_j I_D$ or for "m" parallel strings of "n" series connected diodes as $Q_{semi} = (1-\eta)(nV_j)(mI_D)$. Since a diode exhibits an on-state forward voltage V_j when conducting current I_D , any excess voltage supplied by the photonic drive circuit above the required level also produces extra heat in the amount $Q_{drive} = (V_{drive} - V_j) I_D$ per device (or for an array of m*n devices $Q_{drive} = (nV_{drive} - nV_j)(mI_D)$ where nV_{drive} is the total driver voltage and nV_j is the series sum of diode forward voltages. Generated heat may be released in a PBM controller (requiring a fan to prevent overheating) or may occur in a LED pad contacting the skin.

The final power loss mechanism is the photon flux absorbed in the intervening cutaneous and fascia tissue in the amount $Q_{tiss} = (1-\Psi(x)) P_\lambda$ where for an array of m-by-n devices surface power $P_\lambda = \eta(mI_D)(nV_j)$. Because of the biphasic nature of PBM, the high brightness light absorbed in upper layers of tissue inhibits beneficial PBM, turning instead into kinetic vibration (heat). Overdosing the skin layers does not harm tissue, but it also doesn't benefit it. Total heat generated in driving a parallel-series array of m-by-n devices is then the sum of all component losses, or

$$\begin{aligned} Q_{tot} &= mn(Q_{semi} + Q_{drive} + Q_{tiss}) \\ &= mnI_D V_j \left(\frac{V_{drive}}{V_j} - \eta \Psi(x) \right) \\ &= P_\lambda \left(\frac{V_{drive}}{\eta V_j} - \Psi(x) \right) \end{aligned}$$

where the total input power is $P_{in} = (nV_{drive})(mI_D)$. As expected, increasing the voltage overdrive or decreasing efficiency η increases waste heat Q_{tot} for a given delivered optical power P_λ . Regardless if they are LED or LD emitters, waste heat, not the optical maximum permissible exposure (MPE) criteria, limits the maximum optical power P_λ of a source.

Absorption. Promulgated by device manufacture advertising, numerous misconceptions persist regarding photobiomodulation, especially those discussing deep-tissue PBM therapy. Most notably a misbelief that higher power light should penetrate deeper (because laser light carries more energy) stems from a misapplication of Newtonian classical mechanics to quantum phenomena. Optical power P_λ does not describe the quantized energy of any single photon, but only measures the total

number of photons being emitted in time, i.e. brightness. In non-ablative processes, laser power does not decide photon penetration depth^{150, 151}, just the quantity of photons emitted over time. Instead, penetration depth is probabilistic¹⁵² based on wavelength λ (as per Planck-Einstein) and absorption properties of intervening tissues, not incident power P_λ .

That said, higher power lasers appear to go deeper because they deliver a greater number of photons to tissue more rapidly. In other words, given that $P_{\text{trgt}}(x) = \Psi_{\text{trgt}}(x) P_\lambda$, an increase in the surface brightness P_λ necessarily increases deep tissue irradiance $P_{\text{trgt}}(x)$ proportionally, even for short pulsed transients. The maximum surface brightness P_λ is however limited by skin temperature. Delivering repeated high-power pulses requires longer intervening intervals for heat redistribution, needed to cool off. By contrast, lower power pulses deliver light more slowly but require less cooling time. Since average (not peak) power sets both PBM dose and skin temperature, lasers cannot safely supply a higher average power or dose than LEDs. Moreover, extremely short pulse durations may even reduce penetration depth¹⁵³ whenever photons lack adequate time to traverse intervening biotissue layers to reach a target organ.

Coherency. Another point of contention for over thirty years is the role of light coherency in PBM. Once light enters the skin, biophysical material properties and scattering dominate photon propagation, not wave interference. According to Chen et al¹⁵⁴ coherency does not play significant part in beam spreading. Noting that biotissue includes structural inhomogeneities on the order of light wavelengths, the authors conclude “decoherence of the beam due to the biotissue can occur within micron-like distances.” As such, the benefit of laser light coherency is, in the most optimistic interpretation, limited to upper cutaneous layers. Other papers suggest if coherence is present, it confers no discernable photobiological benefit^{96, 102, 155}. Even advocates of purported benefits of laser interference patterns called “speckles” acknowledge spatial coherence of an illuminating beam is lost to fluid flows¹⁵⁶ and blood perfusion¹⁵⁷ in biological tissue, meaning coherency is relegated at most to the dermis, playing no role in deep-tissue PBM needed in the treatment of COVID-19.

Monochromaticity. Another contested topic in photobiomodulation is the role and importance of monochromatic light. Specifically light sources can be divided into three general categories, namely

broadband, narrow-band (quasi-monochromatic), and monochromatic light.

The sun (and numerous lamps) releases a broad spectrum of wavelengths ranging from far-infrared to ultraviolet. Known benefits of sunlight include improved immunity from cutaneous production of vitamin D, ionization (disinfection) of skin-borne pathogens (including coronaviruses), release of nitric oxide from epithelial stores (improving cardiovascular health), regulation of circadian rhythms, stress reduction, and a general feeling of well-being. Unfortunately, sunlight also includes ionizing radiation known to cause skin cancer. Excessive exposure to far infrared (FIR) radiation is also known to dehydrate tissue, damage skin collagen, and cause premature aging.

The biggest problem with sunlight is only a small portion of its energy is radiated at medically beneficial wavelengths, a minute fraction of its vast spectral emissions. For example, delivering a useful dose of red and NIR light from sunlight requires a patient to also absorb excessive amounts of mid and far infrared EMR, with the risk of overheating. Reducing total exposure to avoid hyperthermia means the delivered dose of therapeutic wavelengths will become too low to stimulate PBM, especially in deep tissue.

A better alternative is to employ a narrow-spectrum emitter (a LD or LED) to deliver most energy at a specific range of wavelengths. If more than one wavelength is required the various colors can be administered sequentially rather than concurrently. Applicable for both lasers and LEDs, applying one-color at-a-time maximizes the therapeutic dose for each session while minimizing unwanted heating effects, thereby shortening treatment times.

Comparing LEDs and LDs however reveals that laser light is purely monochromatic having a precise wavelength, $\lambda \pm 1$ nm while LEDs exhibit spectra which is not. Instead, typical LED emissions span a 70 nm wide band, symmetrically surrounding a center value as $\lambda \pm 35$ nm. In photochemistry, a broader spectrum source is able to stimulate more reactions than a single pure wavelength can. This principle is best understood by considering the transmembrane protein cytochrome-c (and its chromophore cytochrome-c oxidase), key units in the mitochondrial electron transport chain.

Specifically, Karu^{158, 159, 160} and others¹⁶¹ confirmed that cytochrome-c exhibits an *action spectrum* comprising four distinct peaks occurring at different wavelengths. Action spectra differ from simple optical absorption as it identifies wavelengths where photochemical reactions invoke metabolic or physiological change. As reported,

observed mitochondrial action spectra directly affects cellular metabolism including DNA and RNA synthesis, RNA transcription, protein synthesis, and protein attachment. Various action spectra have been identified in red (613-623 nm), far red (667-684 nm) and near infrared regions including a first NIR band (750-772 nm), and a second longer NIR band (813-845 nm). These spectra, covering 80 nm in aggregate, are found to be associated with distinct oxidation states of copper active in metabolic processes.

Capable of 70-nm wide spectral emissions, two LEDs are able to entirely match mitochondrial action spectra in both red bands and in one NIR band, thereby maximizing LED energy delivery to cytochrome-c chromophores. Monochromatic LEDs by contrast, can only stimulate a tight 4-nm spectral width, less than 3% of LEDs. Moreover, since lasers operate at only precise wavelengths and cannot be tuned, there is no guarantee their emitted wavelengths will overlap and activate primary absorption peaks of cytochrome-c chromophores. From this perspective, a LED's broader spectrum is advantageous over purely monochromatic laser light.

Pulsing. The majority of PBM systems in use today are not continuous wave, but instead involve pulsed light. Numerous advantages of pulsed PBM have been reported ¹⁶² including increased mitochondrial metabolism, ROS generation, ATP production, stem cell activity ¹⁶³; greater depth penetration ¹⁶⁴; accelerated wound healing and attenuation of proinflammatory markers ¹⁶⁵; as well as increased Ca^{2+} concentrations and autophagy of melanoma cells ¹⁶⁶.

Pulsing at certain frequencies is also reported to improve *tissue-specific* PBM efficacy in bone growth ¹⁶⁷; enhancing neurological function ¹⁶⁸; treating oral mucositis ¹⁶⁹, and improving outcomes of embolic stroke recovery ¹⁷⁰. Pulsing also provides the ability to regulate PBM dose, average power, and skin temperature. While frequency dependent mechanisms of PBM are not fully understood mechanistically, reports confirm specific pulse frequencies exhibit more pronounced effects than others. Other studies suggest that pulsed light (laser or LED) penetrates deeper than continuous wave ^{171, 172} a phenomena unaccounted for by Monte Carlo analysis and potentially responsible for observed discrepancies between simulation and measurement.

Using pulse width modulation (PWM), alternating durations of high brightness light emission are followed by brief intervals of darkness before repeating. By controlling the respective on

and off times t_{on} and t_{off} as a fraction of a clock period $T_{\phi} = t_{on} + t_{off}$, the average irradiance and skin temperature can be set independently from the peak brightness of the light source. For example, by halving on-time within a fixed clock period, LED brightness can be doubled without affecting the average irradiance P_{λ} . Defined by the relation $D = t_{on} / T_{\phi}$, the duty factor D provides a dynamic means to control both average brightness and skin temperature.

Although most commercial photonic applications (such as HDTV backlights and lamp dimmers) use fixed frequency PWM, in deep tissue PBM it is beneficial to modulate light pulse frequency in accordance with the physiological mechanisms of the targeted organ. This requires controlling both on-time t_{on} and pulse frequency f_{ϕ} . Since pulse frequency is the reciprocal of the clock period $f_{\phi} = 1/T_{\phi}$ then $D = t_{on} f_{\phi}$. The targeted deep-tissue irradiance $P_{trgt}(x)$ is defined by

$$P_{\lambda}/A = D\eta V_j \left(\frac{I_D}{A} \right) = [t_{on} f_{\phi}] \left[\eta V_j \left(\frac{I_D}{A} \right) \right]$$

$$P_{trgt}(x)/A = \Psi_{trgt}(x) (P_{\lambda}/A)$$

where LED on-time t_{on} , pulse frequency f_{ϕ} and diode current I_D are controlled by photonics and where $\Psi_{trgt}(x)$, η , and V_j (as a function of I_D) are determined by material properties.

As shown in **Figure 5**, a sequence of alternating red and near infrared pulses applied to tissue results in a asymptotic rise in skin temperature ¹⁷³. The maximum skin temperature is self-limiting from homeostatic temperature regulation (blood perfusion, sweating, HR) and varies by individual with a peak temperature of 42.8 °C for a fixed 50% duty factor. Measurements also confirm a 5% reduction in duty factor results in a 1 °C lowering of skin temperature.

While the average irradiance for red LEDs is 8.5 mW/cm², a higher flux rate for NIR LEDs of 13.5 mW/cm² produces the same steady-state temperature, supporting the premise that near infrared light penetrates epithelium to greater depths and results in a lower volumetric heat density than red light. These power densities are far below the maximum permissible exposure (MPE) levels of 200 mW/cm² for visible light and 730 mW/cm² for infrared ¹⁷⁴. Note also that because the clock period T_{ϕ} is dynamically changing, maintaining a constant duty factor in variable frequency photonics follows the relation $D = t_{on} f_{\phi}$.

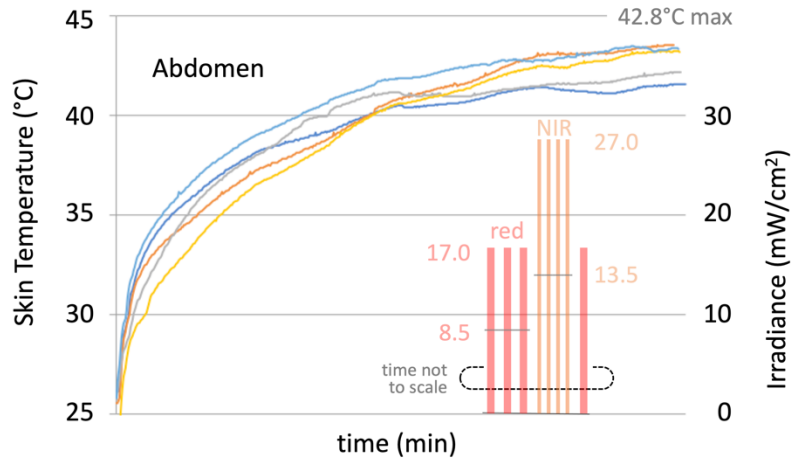


Figure 5. Graph of several patient’s skin temperature in response to a variable frequency pulse string of alternating red and NIR light at a fixed 50% duty factor with average irradiances of 8.5 mW/cm² and 13.5 mW/cm² respectively. Pulse chain (inset) is exemplary (time axis not drawn to scale). Graphic adapted from ¹⁷³.

Fluence (Dose, Energy). In PBM, fluence E measured in Joules (or E/A measured in J/cm^2) represents the energy equivalent to the therapeutic dose of a PBM session, technically defined as the time integral of irradiance. In discrete form, the total deep-tissue fluence (at target depth x) is the sum of the flux of a number of sequential cycles of LED wavelengths, diode currents, pulse frequencies, and step durations T_i given by

$$E_x/A = \sum_{i=1}^z [\Psi_i(x) P_{\lambda_i}/A] T_i$$

where the sum of i -steps of time T_i is the total treatment time T_{tmnt} . For a session of repeated pulses

of a single wavelength λ_1 , the total fluence on the skin’s surface is then simply the multiplicative product of the average surface irradiance P_{λ_1}/A and the total treatment time T_{tmnt} , or $E_0/A = (P_{\lambda_1}/A)T_{tmnt}$. Since the skin is not the PBM target, deep tissue fluence is scaled by the transmission coefficient $\Psi_{trgt}(x)$ whereby $E_x/A = \Psi_{trgt}(x)(P_{\lambda_1}/A)T_{tmnt}$. This equation is graphically illustrated in **Figure 6** for red and NIR light at varying values of $\Psi_{trgt}(x)$ at 1%, 3%, and 5% of the surface flux.

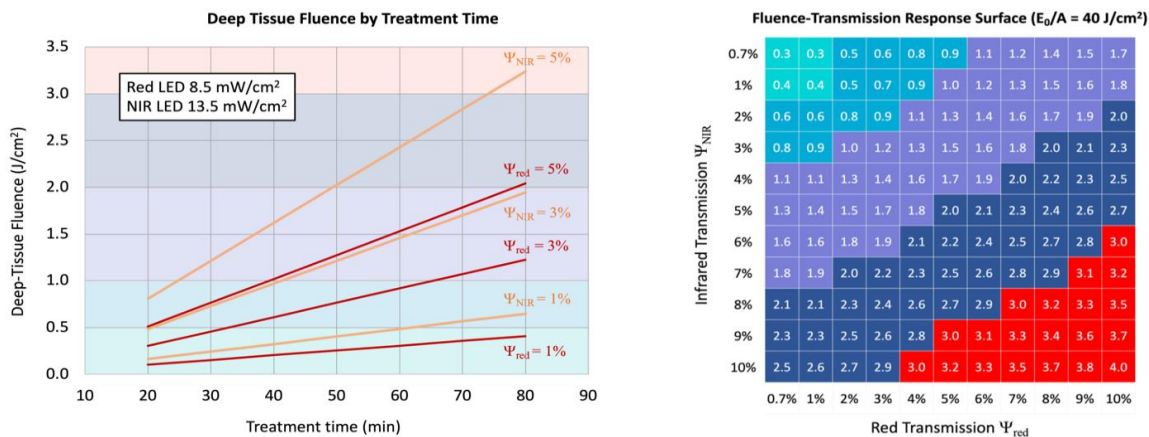


Figure 6. Graph (on left) represents deep-tissue fluence E_x/A (in J/cm^2) of red and NIR therapy by treatment time varied parametrically for transmission coefficients Ψ_{trgt} of 1%, 3%, and 5%. The 3D response surface (on right) illustrates the total aggregate dose of a 1-hour session comprising an even-duration of alternating red and NIR light as a function of red and NIR transmission coefficients Ψ_{trgt} . Fluence calculations are based

on surface irradiances P_{λ}/A of 8.5 mW/cm² and 13.5 mW/cm² for red and NIR light respectively and surface dose of 40 J/cm².

Bias conditions for red LEDs comprise 17 mW/cm² pulses at 50% duty factor having an average power of $P_{\lambda,red} = 8.5$ mW/cm². Bias conditions for NIR LEDs comprise 27 mW/cm² pulses at 50% duty factor with average power $P_{\lambda,NIR} = 13.5$ mW/cm². Analysis reveals a 1% transmission factor (e.g. on the abdomen or atop thick adipose layers) requires more than one-hour treatments to meet a minimum recommended therapeutic dose of 0.5 J/cm². At 3% transmissivity (or better) e.g. treating the lungs or liver, 30 minute treatments easily achieve PBM target fluences. For 5% transmission (when treating the sinuses and AEC), 30 minute fluences range from 0.8 to 1.2 J/cm².

In therapies comprising the alternating application of red and NIR light, separate wavelength fluences are additive where the total dose is given by

$$E_x/A = \left[\Psi_{red}(x) \frac{P_{\lambda,red}}{A} \right] T_{red} + \left[\Psi_{NIR}(x) \frac{P_{\lambda,NIR}}{A} \right] T_{NIR}$$

with red and NIR light treatment times T_{red} and T_{NIR} respectively. At $x = 0$ where $\Psi_{red} = \Psi_{NIR} = 100\%$, the foregoing equation becomes $E_0/A = (P_{\lambda,red}/A)T_{red} + (P_{\lambda,NIR}/A)T_{NIR}$ describing the total fluence on the skin surface. If we assume $T_{red} = T_{NIR} = 30$ min for a one-hour PBM session, the surface flux becomes $E_0/A = (15.3 + 24.3) \text{ J/cm}^2 = 39.6 \text{ J/cm}^2$. Because of attenuation, a higher surface dose is required in order to deliver suggested fluences to deep tissue and organs¹⁷⁵.

By parametrically varying the red and NIR transmission coefficients Ψ_{red} and Ψ_{NIR} to simulate different pad placements and organs targets, deep-tissue PBM fluence can be represented as a 3D response surface (see **Figure 6**). All fluences shown are area-normalized with units of J/cm². For clarity, color graphical bands divide fluences into ranges of total dose including $E_x/A < 0.5$ (green); 0.5-to-1.0 (teal); 1.0-to-2.0 (violet), 2.0-to-3.0 (blue); and 3.0-to-4.0 (red). Although the graph is not symmetric because of higher NIR LED output power, only transmissivities below 1% fail to meet the minimum target^{176, 177} of 0.5 J/cm². The energy shortfall can be adjusted by increasing the time of a therapy session to 80 minutes.

Biphasic Response. Countless studies confirm the photobiomodulation is governed by the Arndt-Schultz curve^{178, 179, 180}, a response surface of efficacy as function of irradiance (i.e. power

density in mW/cm²) and fluence (i.e. energy dose in J/cm²) revealing an optimum set of conditions for stimulating PBM. Excessive irradiance and fluences cause an inhibition of photobiomodulation and may altogether cancel the benefit of a treatment. Provided skin temperature is maintained at a safe level (below 43°C), an energy “overdose” during a PBM treatment has no known detrimental impact on health. This intrinsic safety characteristic is important in deep-tissue PBM where epithelial tissue overlying a PBM targeted organ necessarily absorbs a higher dose than the organ itself. Provided the organ receives a dose in the proper range, PBM benefits are manifest within the tissue target despite power losses in intervening dermal tissue.

The Arndt-Schultz curve is asymmetric with respect to energy. Fluences below a PBM minimum threshold may fail to stimulate a noticeable physiological effect or beneficial outcome. The threshold for minimum irradiance, however, is less pronounced as photon penetration depth is not a function of power. To compensate, a lower irradiance light source can be applied for longer treatment time to reach the target dose¹⁶⁷ provided the treatment time is reasonable. In essence deep-tissue PBM of visceral organs can employ longer session times in order to compensate for lower irradiance levels resulting from intervening tissue absorption. As red and NIR light are non-ionizing, no damage occurs in epithelium, even for extended duration therapy sessions and high PBM fluences. The ability to perform deep-tissue transdermal and transcranial PBM without harming epithelial tissue (from overdosing or excessive temperatures) is an essential feature in the treatment of organs, tissue, nerves, and vessels affected by COVID-19.

PHOTOBIMODULATION OF COVID-19

The efficacious application of photobiomodulation in the treatment of acute and long COVID-19 involves a number of considerations involving quantum photobiochemistry; PBM mechanisms of actions, PBM modalities for COVID-19, and patient outcomes therefrom.

Quantum Photobiochemistry. For light absorbed by target tissues impacted by COVID-19 (e.g. epithelium of lungs; sinus tissue and airway epithelial cells (AEC); liver; brain; intestines; reproductive organs; vascular endothelium; nerve tissue, lymph glands; etc.) several photobiochemical processes may result: (i) emission of conduction electrons stimulating electrochemical processes and neurological transduction; (ii) quantized absorption

causing transformational and bonding changes in molecules and enzymes; (iii) quantized stimulation of ion transport through ion channels, ion gates, and ion pumps (including TRP and cytochrome-c oxidase); and (iv) thermal absorption increasing molecular kinetics and vibration. In some cases, a low-energy photon may also be emitted¹⁸¹ but the biochemical role or utility of secondary photon emission (biophotons), if any, is still highly disputed¹⁸².

Among all of these processes, photobiomodulation is believed to depend mostly on the third category, specifically involving ion transport within CCO of the electron-transport chain of mitochondria^{183, 184} involved in ATP generation and release of NO stores¹⁸⁵ especially in the modulation of cytochrome c as a measure of redox change¹⁸⁶. Counter-arguments suggest the important catalytic role of membrane-bound water (category ii) better explain PBM mechanisms¹⁸⁷

especially at wavelengths over 1,000 nm. To better understand the mechanisms of PBM, it is important to consider the requisite energy to stimulate photochemical reactions.

As shown in **Figure 7**, the photons energy of varying wavelengths are contrasted to the intrinsic energy contained in common organic molecules, most notably adenosine triphosphate (ATP) at 0.50 to 0.55 eV. In quantum photobiochemistry, only photons with sufficient energy to stimulate electron state-changes can invoke a photobiochemical response. As depicted photons in the near infrared and red spectrum from 1,400 nm and shorter carry energies over 0.9 eV, enough to catalyze the synthesis of ATP and numerous polypeptides (even after accounting for entropic thermodynamic losses). Although the entire visible spectrum has sufficient energy to induce PBM, only red and infrared light are able to penetrate deep tissue into SARS-CoV-2 infected organs.

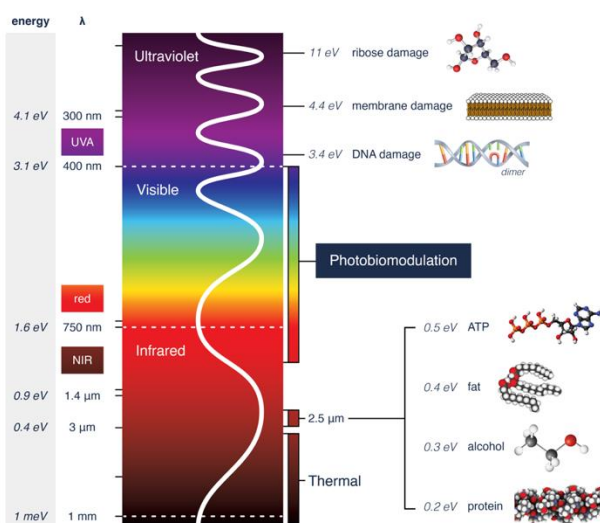


Figure 7. Infrared, visible and ultraviolet portions of electromagnetic spectrum contrasting photon energy to various the energy contained within various biomolecules including ATP illustrating the range of PBM activity. Molecular representations used under licenses from Molecular Science (stock.adobe.com); StudioMolekuul (Shutterstock.com); and public domain works (Mariana Ruiz Villarreal, LadyofHats, Jynto, Ben Mills).

In summary, transdermal and transcranial deep-tissue photobiomodulation requires light to traverse the epithelium, dermal, and subdermal tissues, then penetrate parietal and visceral fascia to reach an organ target. As determined by wavelength (not brightness), photons must carry sufficient energy to exceed minimum requirements to stimulate electron energy transitions in transmembrane bound chromophores. Under principles of thermodynamics and conservation of energy, delivered and absorbed fluence must

exceed the enthalpy of the photochemical reaction product after accounting for losses due to heat and entropy. This minimum energy budget requirement explains why red and NIR exhibit photobiomodulation while FIR (heat) does not.

PBM Mechanisms of Action. The photochemical process by which chromophores respond to light depends not only on a photon's energy, but on photobiochemical reactions specific to the chromophore's molecular biology. Just as SARS-CoV-2 maximizes its opportunities for

infecting multiple organs by binding to the ubiquitous ACE-2 receptor, PBM is fortunate to invoke support from mitochondria, an organelle fundamental to biochemistry present throughout the biosphere and residing in virtually every cell in mammalian and human physiology.

The incredibly complex and diverse roles of mitochondria in the chemistry of eucaryotic life transcend both plant and animal kingdoms. Responsible for the production of adenosine triphosphate (ATP) as the molecular power source for virtually all biochemical reactions, it is mitochondria (not cellular nuclei) that literally manage the birth, life, and death of cells. As an ancient organism predating eukaryotes, mitochondria contain numerous chromophores (many of which remain undiscovered at the time of this writing). Especially suited for directly assimilating light, mitochondria convert photon energy into ATP, promoting cellular replication and ensuring cytological viability while repelling environmental and viral adversaries. As an organelle in plant and animal cells, PBM directly imparts energy into tissue without carbohydrate intermediaries.

The effects of PBM depend on the wavelength of light being absorbed, the pulse frequency of the modulation, and the tissue in which the cells are located. Specifically, photobiomodulation of mitochondria includes direct

and indirect effects on cellular metabolism, respiration, and bioenergetics; cell growth (proliferation, migration, differentiation); cell life cycles (mitosis, autophagy¹⁸⁸, apoptosis, pyroptosis¹⁸⁹, necrosis, phagocytosis); regulation of intracellular ion concentrations (as mediated through TRPs, cation channels, and anion pores); and by homeostatic regulation of divalent calcium (Ca^{2+}), cyclic AMP¹⁹⁰, protein kinases¹⁹¹, and other forms of intracellular signal transduction¹⁷⁷.

One key mitochondrial chromophore in photobiomodulation is cytochrome-c oxidase (CCO), the 4th functional group of transmembrane protein cytochrome-c. As part of the electron transport chain, CCO controls mitochondrial membrane potential (MMP)¹⁹² which in turn regulates ATP production via complex V (an ion channel commonly referred to as ATP synthase¹⁹³). In addition to controlling MMP and ATP synthesis, CCO controls the release of reactive ion species (ROS) and sequestered nitric oxide (NO); cellular communication and retrograde signaling; nuclear transcription factors (NTFs); gene expression (transcription) and epigenetic regulation¹⁹⁴; protein synthesis (translation); protein attachment; and more. Exemplary mechanisms (albeit in abbreviated detail) are represented schematically in **Figure 8**.

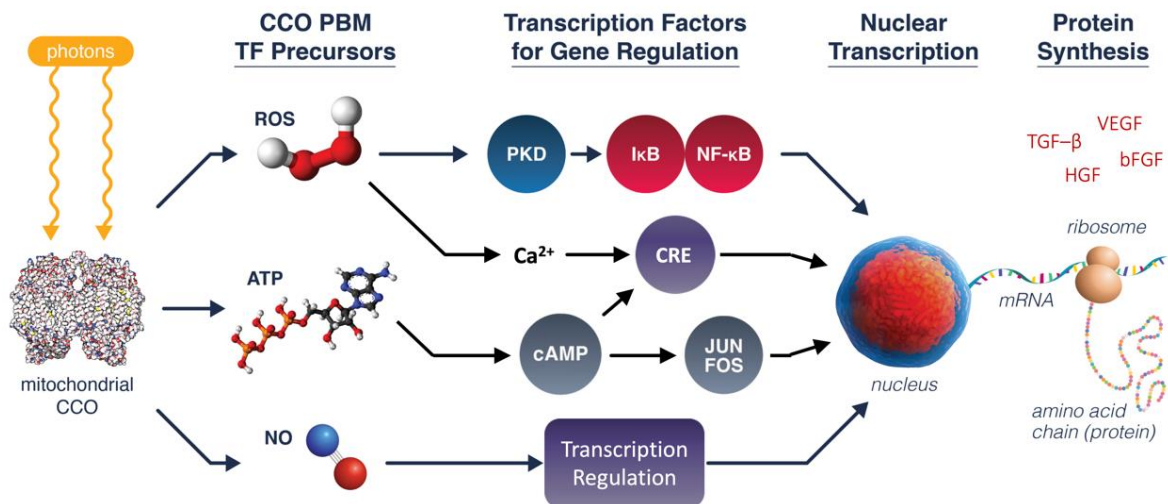


Figure 8. Photobiomodulation of cytochrome-c oxidase includes mechanisms resulting in generation of ATP, ROS, NO and Ca^{2+} influencing signaling, nuclear transcription factors (NTF), transcription, translation, and gene regulation including expression of various growth factors. Organelles and molecular representations used under licenses from Snailstudio (shutterstock.com); PDB-101 (CC 4.0); and public domain works (PixelCraft Design, Ben Mills, Jynto).

As depicted, photobiomodulation of CCO generates and regulates a variety of biomolecules including reactive oxide species (ROS), adenosine

triphosphate (ATP), and nitric oxide (NO). As a self-regulating process the magnitude of photobiomodulation depends on a treated cell's

oxidative stress (and possibly its pH^{159,195}), where compromised cells exhibit a more pronounced photochemical response than healthy ones. Although reactive oxide species are harmful if persistent, in bursts of limited duration they perform a protective function of an anti-infective at the molecular level. Other effects of ROS release involve cellular signaling stimulating nuclear transcription of immune cells, regulating redox states of NAD⁺/NADH¹⁹⁶ and NADP/NADPH¹⁹⁷, balancing the NADH/FAD redox ratio¹⁹⁸, and adjusting divalent calcium levels in response to prolonged or excessive oxidative stress.

PBM also dissociates sequestered NO from CCO¹⁸⁵ diminishing the molecule's inhibitory regulation of the electron transport chain, and increasing the mitochondrial membrane potential (MMP). A higher MMP promotes greater ion transport through ATP synthase increasing production of ATP, accelerating cellular metabolism, and elevating cyclic AMP levels. MMP also regulates transmembrane ion transport and proton leakage through mitochondrial permeability transition (MPT) pores, mitochondrial inner membrane anion channels (IMAC), and others¹⁹⁷.

Aside from facilitating negative feedback in MMP (voltage) regulation, NO (the smallest signaling molecule) modulates transcription factors binding *cis*-regulatory genes in response to microenvironmental dynamics¹⁹⁹. As such, NO plays a crucial role not only in cellular kinetics, but in endogenous defense against cell stress, hypoxia, and disease states. Anti-infective mechanisms include inhibition of ribonucleotide reductase (suppressing viral replication and proliferation) and upregulation of anti-viral heat shock proteins²⁰⁰.

Beyond their direct photochemical involvement, ROS, NO, and ATP function as precursors to transcription factors controlling blood perfusion, innate and adaptive defense, wound healing, and homeostasis. As shown, PBM induced ROS bursts trigger activation of NF-κB eucaryotic nuclear transcription factors controlling immune and inflammatory response, cellular growth and development, and apoptosis. PBM activation of Jun and Fos genes¹⁸⁶ control transcription through the DNA-regulatory activator protein-1 (AP-1) binding site. Proteins coded by Jun-Fos genes are capable of both stimulatory and inhibitory regulation of transcription.

Aside from its role in tumor suppression, AP-1 is now recognized as a regulator of bone and immune cells, and in managing cytokine expression and B-cell receptor modulation in inflammatory diseases (rheumatoid arthritis, psoriasis, psoriatic arthritis, and COVID-19)²⁰¹. Animal *in vivo* models

of immune response to red and NIR PBM include upregulation of anti-inflammatory cytokines (such as IL-10) and a corresponding decline in mRNA expression of pro-inflammatory cytokines, iNOS, and COX-2²⁰², likely through the NF-κB signaling pathway²⁰³. PBM is also known to upregulate heat shock proteins (HSP) such as Hsp70 known to interfere with viral translation and inhibiting thrombus formation²⁰⁴. Other PBM induced immunity to COVID-19 arises from increased macrophage and microglia activity.

As a potent regulator of innate and adaptive immune cell functions, cAMP (derived from ATP) represents a powerful therapeutic target in the treatment of inflammatory and autoimmune diseases (including acute and long COVID-19) by dynamically balancing pro- and anti-inflammatory mediators^{205,190} including regulation of granulocytes (neutrophils, eosinophils, basophils); dendritic cells; NK cells, macrophages; monocytes, T and B cells; T-cell regulators; and epithelial cells. The modulation of cyclic AMP by cellular Ca²⁺ cations stimulate transcription of T-cells via cAMP-response elements (CRE) through the associated transcription factors CREM and CREB. The CRE targeted transcription factors play key roles in immune function and spermatogenesis (aka survival genes)^{206,207}.

Physiological benefits of CCO PBM include anti-infective mechanisms of ROS and innate immune response; reduced inflammation (via interleukins, macrophages, immunoglobins²⁰⁸; and anti-inflammatory cytokines²⁰⁹) in visceral and respiratory epithelium and in vascular endothelium²¹⁰. The anti-inflammatory benefit of PBM is especially critical in COVID-19 disease to combat hyperinflammation of the lungs and bronchia causing congestion, edema, and hypoxia.

Another unique ability of PBM is improved circulation, a key factor in the treatment of acute and long COVID-19. Deep-tissue PBM treatment of the sinuses, airways, lungs, liver, and spleen dramatically enhances blood perfusion, SpO₂ and tissue oxygenation while reducing blood viscosity²¹¹ and thrombotic risk. Numerous mechanisms are involved in PBM circulation benefits including (i) vasodilation from increased NO levels²¹², (ii) reduced endothelial inflammation²¹⁰, (iii) improved cardiopulmonary oxygen exchange efficiency, (iv) temporary inhibition of platelet activity²¹³, (v) reduced blood viscosity^{211,214}, and (vi) increases in the zeta (ζ) electrokinetic potential on erythrocytes (increasing charge repulsive forces)^{215,216,217}. NIR PBM has also been reported to the osmotic frailty of red blood cells, even during hemodialysis^{218,219}. Another potential (as yet unverified) mechanism is

PBM restoration of normal angiotensin homeostasis, possibly degrading the SARS-CoV-2 spike protein to prevent ACE-2 bonding. Vasodilation is also observed in the glymphatic system of the CNS involving enhanced lymph fluid perfusion ²²⁰.

Other PBM benefits include ATP accelerated tissue repair (including activation of neutrophils, fibroblasts ²²¹, and phagocytes); and regulating adaptive immune response to prevent a cytokine storm. PBM induced wound healing includes fibroblastic proliferation and remodeling of visceral epithelium, reduced inflammation of vascular endothelium, angiogenesis, and removal of cellular debris. PBM has also been used to counter nerve damage in the sinuses, the cranial nerves (including the olfactory and gustatory sensory nerves), and the brain by repairing sensory receptors (ion channels) or by replacing damaged neurons altogether through apoptosis and neurogenesis. The improvement of long COVID symptoms of brain fog, depression, and mental health deficits through transcranial PBM has also been attributed to improved circulation and neural connectivity ²²².

Aside from the role of CCO and mitochondria, other organelles and cells may be involved either directly or indirectly in photobiomodulation including endoplasmic reticulum (ER), stem cells ^{192,195}, and mast cells. Although currently no PBM chromophores have been identified in ribosomes, Golgi apparatus, and various immune cells, their potential involvement cannot be eliminated. Other ion channel chromophores (e.g. opsins) operate at wavelengths outside the transparent optical window and are therefore not candidates for deep-tissue PBM.

Deep Tissue PBM Modalities for COVID-19

PBM Therapy of Acute COVID-19. Given the foregoing analysis, a therapeutic regimen for the safe efficacious treatment of acute and long COVID-19 patients using deep-tissue photobiomodulation was developed. By adapting a therapeutic strategy routinely used in the successful treatment of inflammatory respiratory diseases such as acute respiratory distress syndrome (ARDS) and cardio obstructive pulmonary disorder (COPD), and in treating tenacious autoimmune and immunosuppressive diseases (including lupus, Lyme, RA, and H1N1), the acute disease PBM protocol adopts the principal of concurrently treating the body *systemically* while delivering *tissue-specific* therapy to infected organs, specifically those expressing a high density of ACE-2 receptors.

In acute phase COVID-19 infections, tissue and systemic targets can be treated concurrently

during a single session 60-minute session with a 600 cm² LED pad set placed anteriorly across the lungs, heart, and thymus, and a second pad set 400 cm² pad set positioned across the face and sinuses. Each pad in a pad set contains arrays of red (650 nm) and near infrared (850nm) LEDs contained in reconfigurable 3D bendable aseptic polymeric pads designed to conform to body contours.

To maximize tissue specificity to mucosal tissue of the bronchia and AEC (airway epithelial cells), the PBM therapy employs algorithmically sequenced red and NIR LEDs using variable-frequency pulsed modulation with independent duty-factor based temperature control. PBM therapy may be performed by manually executing a sequence of four separate treatments or alternatively selecting a single fully-automated OneTouch™ session (feature on Applied BioPhotonics Mark II models only). Recommended treatment schedules for acute COVID-19 comprises a one-hour PBM session every other day.

Long COVID PBM Therapy. Post acute COVID or long COVID presents a laundry list of conditions across the full spectrum of physiological systems ^{223, 224}. In particular chronic respiratory symptoms ²²⁵ include persistent dyspnea, coughing, chest pain, pulmonary fibrosis, and various pneumonias (UIP, extrinsic allergic alveolitis) and fever. Bronchial scarring can also require regular or perpetual oxygen supplementation.

Significant deficits in circulatory function are also common. Presentations include chest tightness, numbness, hypertension, stroke, thromboembolism ²²⁶, arrhythmia ²²⁷, myocardial damage, heart failure, myocarditis ²²⁸, and inflammatory heart disease. Heart symptoms persist in 10% of patients with long COVID ²²⁹. Patients with heart-related long COVID also exhibit a 20% decrease in their coronary arteries' ability to vasodilate ²³⁰.

Digestive symptoms of long COVID syndrome ²³¹ include diarrhea, stomach pain, acid reflux, liver dysfunction, acute pancreatitis, irritable bowel syndrome, stomach and intestinal ulcers, and acute kidney injury (AKI). Genitourinary long-COVID symptoms include COVID associated cystitis (CAC) ²³²; lower urinary tract symptoms (LUTS) absent bacterial infection; urinary incontinence (UI); hematuria (urinary blood); acute genital ulcers, lesions, and rashes (with negative exudate bacterial cultures and herpes simplex virus PCR tests) ²³³. Long COVID impact on reproductive organs ²³⁴ includes testicular pain, erectile dysfunction, hypogonadism, and reduced sperm count in biological males; and premature ovarian failure, reduced oocyte quality,

abnormal menstruation and bleeding, and infertility in females.

Reported post COVID neurological manifestations ²³⁵ include chronic pain and neuritis, cognitive deficits, inability to concentrate, brain fog, malaise, confusion, sleep disorders, dizziness, tinnitus, aphasia, and degraded sensory perception (anosmia, ageusia, PVL). Emotional and psychiatric sequelae ²³⁶ may also result including depression, anxiety, and post traumatic stress disorder (PTSD). More recently it was discovered psychological stress is not only a symptom of long COVID but a risk factor ²³⁷.

Treatment of long COVID-19 conditions can be divided into four categories: (i) transdermal PBM of visceral organs, (ii) transdermal PBM of central and peripheral nerves, (iii) transcranial PBM of the brain and cranial neuroendocrine organs, and (iv) systemic PBM. Each category involves a different sequential protocol with specificity for epithelium, endothelium, or nerve tissue. PBM of visceral organ targets include lungs, heart, liver, kidneys, glands, intestines, and reproductive organs.

Nerve therapy used to ameliorate long COVID related neuralgia, muscle cramping, organ pain, paresthesia, neuropathic pain, and fibromyalgia involves pad placement targeting major nerves of the autonomic and somatic nervous systems including the spine, the vagus nerve, and major peripheral nerves (such as the sciatic and lumbosacral plexus nerves). It should be noted viral damage to spinal, cranial, and peripheral nerves can deceptively present symptoms of muscular or organ pain even if the organ itself is undamaged. Transcranial PBM of long COVID employs primarily NIR light using protocols adapted from over a decade of treatment experience for stroke, mTBI-concussion, and Alzheimer's dementia (AD).

Systemic PBM involves modulating the immune, endocrine, and neuroendocrine systems by concurrently stimulating principal organs. By placing three LED pads along the anterior central core (referred to as the Schell central core) from under the throat along the sternum onto the stomach, most significant organs involved in immuno-hormonal regulation can be modulated in a single 60-minute PBM session (including the thymus, thyroid, parathyroid, major lymph nodes, esophagus, trachea, lungs, heart, stomach, liver and spleen). Protocols are discussed in Part II.

COVID-19 Clinical Case Studies

Whole-organ PBM Backstory. In mid-March of 2020 one month after confirmation of COVID-19 disease ²³⁸, Applied BioPhotonics urgently published a newsletter to its community of device owners ²³⁹ proposing an anti-inflammatory

anti-infective protocol for treating the newly isolated SARS-CoV-2 coronavirus with its PBM. Based on extensive experience in treating inflammatory diseases (including SARS, H1N1, COPD, ARDS, and pneumonias), the protocol employed pad placements shown in **Figure 9** delivering concurrent therapy of the sinuses (with two available options) and the immune system (placed along the Schell central core).

However, after a review of pulmonary radiographic data revealed a high degree of multifocal ground glass opacity and dense bilateral peripheral consolidation ²⁴⁰, recommended LED pad orientation on the chest was rotated 90° transversely to maximize coverage of the lungs. The revised PBM protocol underscored for the first time, the importance of *whole-organ* photobiomodulation as a modality to prevent intrabronchial reinfection.

Throughout 2020 in the absence of therapeutics and vaccines hospitals overflowed and symptomatic patients, afraid of visiting hospitals or clinics, sheltered-in-place avoiding public contact at the expense of deferring professional medical care. With the contagion rapidly spreading to front line health care workers, over a dozen physicians and therapists in our community soon contracted COVID-19. Unlike the general population, however, those doctors with experience using deep-tissue PBM were able to perform self-treatment. Following the suggested protocol, reports of favorable outcomes with full recovery in 3-to-5 days defied all expectations.

COVID PBM Case Studies: Soon thereafter, the same community of physicians started performing ambulatory therapy on patients unable or unwilling to seek hospital admission. In accordance with compassionate care standards for medical caregivers, all requesting patients' treatment whether asymptomatic, mildly symptomatic, and severely ill; tested or not; were administered whole-organ deep-tissue PBM therapy free-of-charge. Patients were treated using hands-free application of 3D conforming LED pads while maintaining separate enclosures (with 2-meter-long cabling). As such no doctors became infected delivering this service. The outcome reported in ¹¹¹ showed 50/50 patients recovered from acute symptoms within three days of commencing PBM and with the vast majority of the population recovering fully within 5 days. Untested symptomatic and asymmetric patients in direct contact with COVID infected family members were also treated, none of whom presented active COVID-19 symptoms. Moreover, no PBM treated

patient ever developed long COVID symptoms or required supplemental oxygen.

The results inspired another group of doctors in a Taiwan hospital to repeat the procedure except with the benefits of full diagnostics including x-Rays, blood tests, and

patient monitoring records (oxygen use, vitals). The study similarly ²⁴¹ confirms beneficial outcomes of the test group and contrasts them to patients who did not receive PBM with less favorable outcomes. More details of the Taiwan study are discussed in Part II.



Figure 9. Preliminary LED pad recommendation (as per 14 Mar 2020) for treating COVID-19 with deep-tissue whole organ PBM comprising a anti-infective, anti-inflammatory protocol ²³⁹. After reviewing chest x-Rays, suggested chest pad orientation was rotated by 90° to maximize coverage of the lungs.

PBM of Long COVID Cases. Over 200 patients have received whole-organ deep-tissue PBM therapy for long COVID by doctors and therapists. Treated patients include those experiencing a wide range of metabolic, neurological, and multi-organ syndromes. Reported results of deep-tissue transdermal and transcranial PBM include restored breathing, elimination of COVID-related chronic pain, restored mobility, cessation of brain fog, improvement in memory recall and executive function, recovery of gut health eliminating digestive distress, metabolic improvements with reduced fatigue and malaise, and improved psychological state-of-being. A full description of the work remains unpublished at this time (manuscript in preparation) but a sample of patient cases are included in Part II. The prognosis for the treatment of long COVID is favorable.

DISCUSSION

In the year 2020, the emergence of the highly-transmissible SARS-CoV-2 virus rapidly spread uncontained into a deadly global pandemic. Easily passed through human contact, the poorly understood COVID-19 disease exhibited presentations of a *multisystem inflammatory syndrome* of the respiratory, circulatory, and immune systems, exacerbated by the virion's proclivity for RNA insertion through the ubiquitous

and pervasive ACE-2 receptor (a widely distributed protein critically involved in local homeostatic regulation of angiotensin and organ blood pressure). Without the prospect for inoculation and lacking any known pharmacological interventions to manage the severity of infection, doctors were forced to turn to evidence-based medicine ²⁴² to identify modalities for providing symptomatic relief and compassionate care for families desperately seeking options.

Although not widely available at the time, one such intervention was photobiomodulation, the transdermal application of red and near infrared light already established to exhibit anti-inflammatory, anti-infective, and pro-circulatory properties well matched to the very symptoms COVID-19 manifests. With profoundly successful results in early trials and lacking other therapeutic options, physicians deemed it inappropriate (or even unethical) to deny care to any of their patients seeking PBM treatments. As such, pioneering doctors using photobiomodulation (generally in ambulatory care) to treat COVID-19 during its outbreak, had neither the opportunity nor the volunteers willing to participate in randomized clinical trials by putting a control group at lethal risk.

Later, limited population trials (generally treating newer less lethal variants of the virus) statistically confirmed the benefits of using PBM in

the treatment of COVID-19 in all stages of disease progression ^{243,244,245}. Other larger empirical studies, although lacking any control group, were compelling because of statistical significance with 50 of 50 patients experiencing relief of all acute conditions within 3 days of PBM treatment ¹¹¹, irrespective of the severity of their condition at the time of treatment. Intubated and ventilated patients were not included in the study (as they were hospitalized and unavailable for outpatient treatment). Finally, numerous studies confirm by pulmonary radiography and blood analysis that PBM rapidly results in clearance of lung inflammation and significant declines in inflammatory markers ²⁴¹. These and other trial results are discussed in Part II of this paper.

Unanswered questions in the application of photobiomodulation for treatment of COVID-19 disease therefore focus not on “if” PBM works, but more importantly “how does it work”. As discussed throughout this paper to treat internal organs and glands with deep-tissue PBM (i) light must penetrate

the air-to-skin interface without significant optical power loss (i.e. light incident perpendicular to the skin’s surface); (ii) light must comprise a wavelength in the red and near infrared spectrum in order to traverse cutaneous and fascial tissue to reach visceral organs; (iii) light must carry sufficient energy to modulate mitochondrial CCO and generate ATP (for which red and NIR do); and (iv) the total fluence at depth determined by the product of irradiance and time must be sufficient to invoke a substantial PBM response.

Despite inconsistencies in the reported absorption and scattering properties of various cutaneous, subcutaneous, and fascial layers covering visceral organs, an integrated model of deep tissue fluence and PBM response is presented herein. As shown in **Figure 10**, the model confirms that to achieve a dose exceeding 0.5 J/cm² within the lungs or other visceral organs, a surface fluence of 40 J/cm² is necessary to compensate for the optical attenuation of intervening tissue.

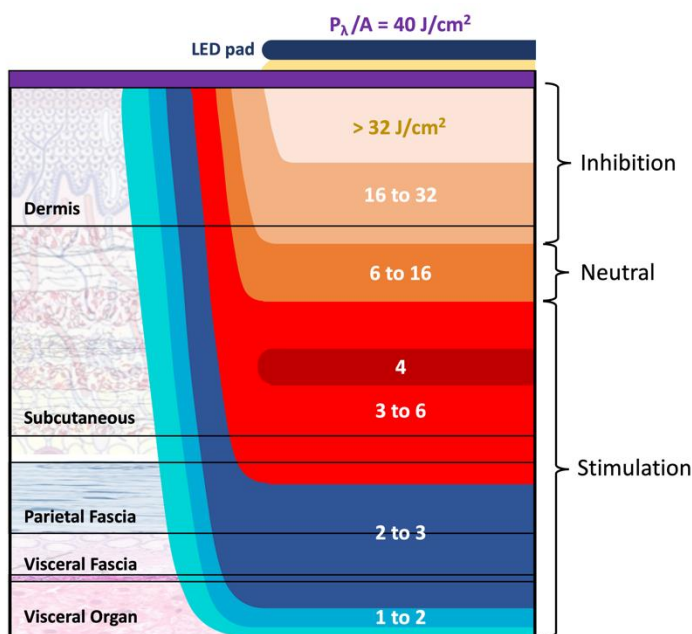


Figure 10. Depth profiles of optical fluence in the integument for a red-NIR blended surface energy of 40 J/cm². In accordance with Arndt-Schultz biphasic response, high doses in the dermis are inhibitory with PBM stimulation occurring deeper in visceral organs and secondarily in the highly vascularized lower subcutaneous tissue layers.

Target surface fluence can be achieved using pulsed light at either high or low duty factors, where the maximum brightness is determined by the time-average or steady-state temperature of the skin being limited to below 43°C, not by peak brightness during diode conduction. As such scanned lasers and LED pads are equally applicable for deep-tissue PBM with the caveat that impinging light must be perpendicular to the skin in order to penetrate subdermally. Practically speaking,

orthogonal illumination means laser scanning angles must be limited to no more than 30° off axis and an LED pad must be bendable in three dimensions to conform to body contours.

Other interesting observations from this study suggest in accordance with the Arndt-Schultz biphasic model, peak PBM activity occurs in the subcutaneous layer populated by blood vessels, thereby conferring an added benefit of reduced endothelial inflammation; lower blood viscosity and

reduced thrombosis; vasodilation; a lowering of local blood pressure; increased SpO₂, and an overall systemic increase in tissue oxygenation. Notice too that epidermal and dermal layers do not participate in or benefit from deep-tissue PBM regimens.

While the prognosis for the use of deep-tissue photobiomodulation in the treatment of acute and long COVID-19 and other inflammatory disease is encouraging, many questions involving the mechanisms within visceral organ epithelium and deep vascularization remain unanswered.

Disclaimers

Richard K. Williams is founder, CEO, president, CTO, and a shareholder of Applied BioPhotonics, Ltd. (ABP) and co-founder and CEO of LightMD, Inc., a member of the ABP group of global affiliates. He is also founder, CEO, and CTO of technology-

innovator Adventive Technology Ltd., and a founding member of HyperSphere.ai and several blockchain DAOs. ABP is a GMP-certified device manufacturer, system specifier, and IP holder of medical devices and PBM therapy products. The author received no financial sponsorship or compensation in the preparation of this article.

Acknowledgments

The author would like to thank Laura E Williams of PixelCraft Design for artistic and graphical production of this work. The author would like to acknowledge Dan Schell of LightMD Inc in the USA, Ken Lin of LightDr in Asia, and Arindam Sarkar of AraLight in the Middle East, Africa, and India for their long-standing support of Applied BioPhotonics and for developing PBM protocols over the last decade, especially during the pandemic.

References

1. 1918 Pandemic (H1N1 virus). *Centers for Disease Control & Prevention*. [Last reviewed 2023 Mar 20]. [\[online\]](#)
2. DeSalvo K, Hughes B, Bassett M, Benjamin G, Fraser M, Galea S, Gracia JN, Howard J. Public health COVID-19 impact assessment: lessons learned and compelling needs. *NAM Perspectives*. 2021 Apr 7. [\[online\]](#)
3. COVID-19 pandemic: what's next for public health? *The Lancet*. 2022 May. [\[online\]](#)
4. Chapter 1. The economic impacts of the COVID-19 crisis. *The World Bank: World Devel Report 2022* [\[online\]](#)
5. Arias E, Tejada-Vera B, M.S., Kochanek KD, Ahmad FB. Provisional life expectancy estimates for 2021. *NVSS Vital Statistics Rapid Release*. 2022 Aug. 22. [\[online\]](#)
6. Stein R, Wroth C, Hurt A. U.S. Coronavirus testing still falls short. How's your state doing? *Shots – Health News from NPR*. 2020 May 7. [\[online\]](#)
7. Spencer DJ. COVID-19 Timeline. *CDC Museum: Centers for Disease Control and Prevention*. [Last reviewed 2022 Aug 16]. [\[online\]](#)
8. COVID-19 pandemic triggers 25% increase in prevalence of anxiety and depression worldwide. *World Health Org*. 2022 Mar 2. [\[online\]](#)
9. Panchal N, Kamal R, Cox C, Garfield R. The implications of COVID-19 for mental health and substance use. *KFF: Kaiser Family Foundation*. 2021 Feb 10. [\[online\]](#)
10. Betthäuser BA, Bach-Mortensen AM, Engzell P. A systematic review and meta-analysis of the evidence on learning during the COVID-19 pandemic. *Nature Human Behavior*. 2023 Jan 30. [\[online\]](#)
11. Oosterhoff M et al. Estimating the health impact of delayed elective care during the COVID -19 pandemic in the Netherlands. *Soc Sci Med*. 2023 Mar; 320: 115658. [\[PubMed\]](#)
12. Gertz AH, Pollack CC, Schultheiss MD, Brownstein JS. Delayed medical care and underlying health in the United States during the COVID-19 pandemic: A cross-sectional study. *Prev Med Rep*. 2022 Aug; 28: 101882. [\[PubMed\]](#)
13. WHO Coronavirus (COVID-19) Dashboard. *World Health Org*. 2023 Feb 21. [\[online\]](#)
14. Troeger C. Just How Do Deaths Due to COVID-19 Stack Up? *ThinkGlobalHealth*. 2023 Feb 15. [\[online\]](#)
15. Endemic COVID-19. *Wikipedia*. [Last reviewed 2023 Feb 23]. [\[online\]](#)
16. Long COVID. *CDC Center for Disease Control and Prevention*. [Last reviewed 2022 Dec 16]. [\[online\]](#)
17. SARS-CoV-1. *Wikipedia*. [Last reviewed 2023 Jan 30]. [\[online\]](#)
18. Mohd HA, Al-Tawfiq JA, Memish ZA. Middle East respiratory syndrome coronavirus (MERS-CoV) origin and animal reservoir. *Virology*. 2016 Jun 3. 13:87 (2016). [\[online\]](#)
19. Roth L. Coronavirus history. *WebMD*. [Last reviewed 2022 Dec 31] [\[online\]](#)
20. Holmes EC, et al. The origins of SARS-CoV-2: A critical review. *Cell*. 2021 Sep 16. 184. ©

- 2021 The Author(s)]. Published by Elsevier Inc. [\[online\]](#)
21. Prince, Smith SL, Radford AD, Solomon T, Hughes GL, Patterson EI. SARS-CoV-2 infections in animals: reservoirs for reverse zoonosis and models for study. *Viruses*. 2021 Mar 17; 13(494). [\[online\]](#)
 22. Ji W, Wang W, Zhao X, Zai J, Li X. Cross-species transmission of the newly identified coronavirus 2019-nCoV. *J Med Virol*. 2020 Apr; 92(4): 433-440. [\[online\]](#)
 23. Valencak TG, Csiszar A, Szalai G, Podlutzky A, Tarantini S, Fazekas-Pongor V, Papp, Ungvari Z. Animal reservoirs of SARS-CoV-2: calculable COVID-19 risk for older adults from animal to human transmission. *GeroScience*. 2021 Oct; 43(5): 2305–2320. [\[online\]](#)
 24. Differential susceptibility of SARS-CoV-2 in animals: Evidence of ACE2 host receptor distribution in companion animals, livestock and wildlife by immunohistochemical characterisation. *Transbound Emerg Dis*. 2022 Jul; 69(4): 2275–2286. [\[online\]](#)
 25. Wei Y, Aris P, Farookhi H, Xia X. Predicting mammalian species at risk of being infected by SARS-CoV-2 from an ACE2 perspective. *Sci Rep*. 2021 Jan 18; 11(1702). [\[online\]](#)
 26. Chitsike L, Duerksen-Hughes P. Keep out! SARS-CoV-2 entry inhibitors: their role and utility as COVID-19 therapeutics. *Viol J*. 2021 Jul 23; 18(154). [\[online\]](#)
 27. Sheridan K. The coronavirus sneaks into cells through a key receptor. Could targeting it lead to a treatment? *Stat*. 2020 Apr 10. [\[online\]](#)
 28. Scientific Brief: SARS-CoV-2 transmission. CDC Center for Disease Control and Prevention. [Last reviewed 2021 May 7]. [\[online\]](#)
 29. Jackson CB, Farzan M, Chen B, Choe H. Mechanisms of SARS-CoV-2 entry into cells. *Nature Rev Mol Cell Bio*. 2022 Jan; 23: 3-20. [\[online\]](#)
 30. Turner AJ. Chapter 25 – ACE2 cell biology, regulation, and physiological functions. *NIH National Lib Med The Protective Arm of the Renin–Angiotensin System (RAS)*. 2015 Apr 24: 185-189. [\[PubMed\]](#)
 31. Knapp S. Aldosterone. *Bio Dictionary*. 2020 Oct 27. [\[online\]](#)
 32. Angiotensin-converting enzyme 2. *Wikipedia*. [Last reviewed 2022 Feb 12]. [\[online\]](#)
 33. Sriram K, Insel P, Loomba R. What is the ACE2 receptor, how is it connected to coronavirus and why might it be key to treating COVID-19? The experts explain. *The Conversation*. 2020 May 14. [\[online\]](#)
 34. Samavati L, Uhal BD. ACE2, Much more than just a receptor for SARS-COV-2. *Front Cell Infect Microbio*. 2020 Jun 5; 10. [\[online\]](#)
 35. Scialo F, Daniele A, Amato F, Pastore L, Matera MG, Cazzola M, Castaldo G, Bianco A. ACE2: The major cell entry receptor for SARS-CoV-2. *Lung*. 2020 Nov 10; 198(6): 867–877. [\[online\]](#)
 36. Lubbe L, Cozier GE, Oosthuizen D, Acharya KR, Sturrock ED. ACE2 and ACE: structure-based insights into mechanism, regulation and receptor recognition by SARS-CoV. *Clin Sci (London)*. 2020 Nov 4; 134(21): 2851–2871. [\[PubMed\]](#)
 37. Sriram K, Insel PA. A hypothesis for pathobiology and treatment of COVID-19: The centrality of ACE1/ACE2 imbalance. *British J Pharma (BJP)*. 2020 Nov; 177(21): 4825-4844. [\[online\]](#)
 38. Daniell H, Nair SK, Shi Y, Collman RG, Laudanski K, Bar KJ. Decrease in angiotensin-converting enzyme activity but not concentration in plasma/lungs in COVID-19 patients offers clues for diagnosis/treatment. *Molecular Ther Meth Clinical Dev*. 2022 Sep; 26: 266-278. [\[online\]](#)
 39. Masre SF, Jufri NF, Ibrahim FW, Raub SHA. Classical and alternative receptors for SARS-CoV-2 therapeutic strategy. *Rev Med Virol*. 2021 Sep; 31(5). [\[PubMed\]](#)
 40. Leonardi A, Rosani U, Brun P. Ocular surface expression of SARS-CoV-2 receptors. *Ocular Immun Inflam*. 2020 Jul 3; 28(5): 735-738. [\[PubMed\]](#)
 41. Barnett BP, Wahlin K, Krawczyk M, Spencer D, Welsbie D, Afshari N, Chao D. Potential of ocular transmission of SARS-CoV-2: A review. *Vision*. 2020 Sep 1; 4(3): 40. [\[PubMed\]](#)
 42. Armstrong L, Collin J, Mostafa I, Queen R, Figueiredo FC, Lak M. In the eye of the storm: SARS-CoV-2 infection and replication at the ocular surface? *Stem Cells Trans Med*. 2021 Mar 12; 10: 976–986. [\[online\]](#)
 43. Bohn MK, Hall A, Sepiashvili L, Jung, Shannon Steele S, Adeli K. Pathophysiology of COVID-19: Mechanisms underlying disease severity and progression. *Physiology (Bethesda)*. 2020 Sep 1; 35(5): 288–301. [\[online\]](#)
 44. Bartas M, Volná A, Beaudoin CA, Poulsen ET, Červeň J, Brázda V, Špunda V, Blundell TL, Pečinka P. Unheeded SARS-CoV-2 proteins? A deep look into negative-sense RNA. *Brief Bioinform*. 2022 May 13; 23(3): 1-10. [\[PubMed\]](#)
 45. Lauer SA, et al. The incubation period of coronavirus disease 2019 (COVID-19) from publicly reported confirmed cases: estimation

- and application. *Ann Intern Med.* 2020 May 5; 172(9): 577-582. [online]
46. Hersh E, Seladi-Schulman J. After exposure to the coronavirus, how long before symptoms appear? *Healthline.* [Last reviewed 2021 Dec 3]. [online]
 47. Ma Q, Liu J, Liu Q, Kang L, Liu R, Jing W, Wu Y, Liu M. Global percentage of asymptomatic SARS-CoV-2 infections among the tested population and individuals with confirmed COVID-19 diagnosis. *JAMA Netw Open.* 2021 Dec; 4(12). [PubMed]
 48. Shang W, Kang L, Cao G, Wang Y, Gao P, Liu J, Liu M. Percentage of asymptomatic infections among SARS-CoV-2 Omicron variant-positive individuals: a systematic review and meta-analysis. *Vaccines (Basel).* 2022 Jul; 10(7): 1049. [online]
 49. Hall SM, et al. Comparison of anterior nares viral loads in asymptomatic and symptomatic individuals diagnosed with SARS-CoV-2 in a university screening program. *PLOS One.* 2022 [© 2022 Hall et al.] 2022 Jul 13; 17(7). [online]
 50. Shirbhate E, Jaiprakash Pandey J, Patel VK, Kamal M, Jawaid T, Gorain B, Kesharwani P, Rajak H. Understanding the role of ACE-2 receptor in pathogenesis of COVID-19 disease: A potential approach for therapeutic intervention. *Pharma Rep.* 2021; Jun 27 73(6): 1539–1550. [online]
 51. Mizrahi B, et al. Longitudinal symptom dynamics of COVID-19 infection. *Nat Comm.* 2020 Dec 4; 11(1): 6208. [online]
 52. Jordan RE, COVID-19: Risk factors for severe disease and death. *BMJ* 2020 Mar 26; 368. [online]
 53. Chen Y, Wang J, Liu C, Su L, Zhang D, Fan J, Yang Y, Xiao M, Xie J, Xu Y, Li Y, Zhang S. IP-10 and MCP-1 as biomarkers associated with disease severity of COVID-19. *Molec Med.* 2020 Oct 29; 26(97). [online]
 54. Devang N, Sreelatha S, Mamatha BV. Assessment of inflammatory markers and their association with disease mortality in severe COVID-19 patients of tertiary care hospital in South India. *Egyptian J Bronc.* 2022 Nov 4; 16(55). [online]
 55. Maamar M, Artime A, Pariente E, Fierro P, Ruiz Y, Gutiérrez S, Tobalina M, Díaz-Salazar S, Ramos C, Olmos JM, Hernández JL. Post-COVID-19 syndrome, low-grade inflammation and inflammatory markers: a cross-sectional study. *Current Med Res Opinion.* 2022 Mar 9; 1–9. [PubMed]
 56. Balta S, Balta I. COVID-19 and inflammatory markers. *Curr Vasc Pharma.* 2022 May 13; 20(4): 326-332. [PubMed]
 57. Sanyal S. How SARS-CoV-2 (COVID-19) spreads within infected hosts — what we know so far. *Emerg Top Life Sci.* 2020 Dec 11; 4(4): 383-390. [PubMed]
 58. Naji HS. Cytokine storm of SARS-CoV-2, the virus that causes COVID-19. *EJMED, Euro J Med Health Sci.* 2020 May 11; 2(3). [online]
 59. Ragab D, Salah Eldin S, Taeimah M, Khattab R, Salem R. The COVID-19 cytokine storm: What we know so far. *Front Immunol.* 2020 Jun 16; 11: 1446. [PubMed]
 60. Fajgenbaum DC, June CH. Cytokine storm. *N Engl J Med.* 2020 Dec 3; 383(23): 2255–2273. [PubMed]
 61. Ho S. Inflammation and immunity troubles top long COVID suspect list. *WebMD.* 2023 Feb 1. [online]
 62. Ferdinands J, et al. Waning of vaccine effectiveness against moderate and severe COVID-19 among adults in the US from the VISION network: test negative, case-control study. *BMJ.* 2022 Oct 3; 379. [online]
 63. Wright BJ, Tideman S, Diaz GA, French T, Parsons GT, Robicsek A. Comparative vaccine effectiveness against severe COVID-19 over time in US hospital administrative data: a case-control study. *Lancet Respir Med.* 2022 Jun; 10(6): 557–565. [PubMed]
 64. Katella K. Omicron, Delta, Alpha, and more: what to know about the coronavirus variants. *Yale Med.* [Last reviewed 2023 Feb 3]. [online]
 65. Wang Q, et al. Key mutations on spike protein altering ACE2 receptor utilization and potentially expanding host range of emerging SARS-CoV-2 variants. *J Med Virol.* 2022 Sep 22; 95(1). [online]
 66. Robinson PC, Liew DFL, Tanner HL, Zitzmann N. COVID-19 therapeutics: Challenges and directions for the future. *PNAS.* 2022 Apr 6; 119(15). [online]
 67. Stein SR, et al. SARS-CoV-2 infection and persistence in the human body and brain at autopsy. *Nature.* 2022 Dec 14; 612: 758–763. [online]
 68. O'Mary L. Autopsies show COVID virus invades entire body. *WebMD.* 2023 Jan 9. [online]
 69. Abbasi J. The COVID heart— One year after SARS-CoV-2 infection, patients have an array of increased cardiovascular risks. *JAMA.* 2022 Mar 22; 327(12): 1113-1114. [online]
 70. Davis HE, McCorkell L, Vogel JM, Topol EJ. Long COVID: major findings, mechanisms and

- recommendations. *Nat Rev Micro*. 2023 Jan 13; 21: 133-146. [[online](#)]
71. Freitas de Freitas L, Hamblin MR. Proposed mechanisms of photobiomodulation or low-level light therapy. *IEEE J Sel Top Quantum Electron*. 2016 May-Jun; 22(3): 7000417. [[PubMed](#)]
 72. Amaroli A, Ferrando S, Benedicenti S. Photobiomodulation affects key cellular pathways of all life-forms: considerations on old and new laser light targets and the calcium issue. *Photochem Photobiol*. 2019 Jan; 95(1): 455-459. [[PubMed](#)]
 73. Wang X, Tian F, Soni SS, Gonzalez-Lima F, Liub H. Interplay between up-regulation of cytochrome-c-oxidase and hemoglobin oxygenation induced by near-infrared laser. *Sci Rep*. 2016; 6: 30540. [[PubMed](#)]
 74. Stasko N, et al. Visible blue light inhibits infection and replication of SARS-CoV-2 at doses that are well-tolerated by human respiratory tissue. *Sci Rep*. 2021 Oct. 11(1): 20595. [[online](#)]
 75. Pick E. Reactive oxygen species are at the heart of innate immunity. *Research Outreach*. 2020 Oct 2. [[online](#)]
 76. Amini MA, Karimi J, Talebi SS, Piri H. The association of COVID-19 and reactive oxygen species modulator 1 (ROMO1) with oxidative stress. *Chonnam Med J*. 2022 Jan 25; 58(1): 1–5. [[PubMed](#)]
 77. Lacy P, Stow JL. Cytokine release from innate immune cells: Association with diverse membrane trafficking pathways. *Blood*. 2011 Jul 7; 118(1): 9-18. [[online](#)]
 78. Aguida B, et al. Infrared light therapy relieves TLR-4 dependent hyper-inflammation of the type induced by COVID-19. *Comm Integ Bio*. 2021; 14(1): 200–212. [[online](#)]
 79. Marashian SM, Hashemian M, Pourabdollah M, Nasser M, Mahmoudian S, Reinhart F, Eslaminejad A. Photobiomodulation improves serum cytokine response in mild to moderate COVID-19: the first randomized, double-blind, placebo controlled, pilot study. *Front Immunol*. 2022 Jul 8; 13(929837). [[online](#)]
 80. Hanna R, Dalvi S, Sălăgean T, Bordea IR, Benedicenti S. Phototherapy as a rational antioxidant treatment modality in COVID-19 management; new concept and strategic approach: critical review. *Antioxidants (Basel)*. 2020 Sep 16; 9(9): 875.
 81. Fekrazad R. Photobiomodulation and antiviral photodynamic therapy as a possible novel approach in COVID-19 management. *Photobiomodulation, Photomed, Laser Surgery*. 2020 May 19; 38(5). [[online](#)]
 82. Bathini M, Raghushaker CR, Mahato KK. The molecular mechanisms of action of photobiomodulation against neurodegenerative diseases: a systematic review. *Cellular Molec Neurobio*. 2020 Dec 10; 42: 955–971. [[online](#)]
 83. Newsom P. Photobiomodulation as a treatment modality for COVID-19 sequelae. *Townsend Letter*. 2023 Mar 7. [[online](#)]
 84. Hamblin MR. Photobiomodulation or low-level laser therapy. *J Biophotonics*. 2016 Dec; 9(11-12): 1122–1124. [[PubMed](#)]
 85. The Nobel Prize in Physiology or Medicine 1903. *The Nobel Prize*. [[online](#)]
 86. *Annus mirabilis* papers. *Wikipedia*. [last reviewed 2023 Jan 1]. [[online](#)]
 87. Niaz M, Klassen S, McMillan B, Metz D. Reconstruction of the history of the photoelectric effect and its implications for general physics textbooks. *Sci Educ*. 2010 Jan 14; 94: 903-931. [[online](#)]
 88. The Nobel Prize in Physics 1921. *The Nobel Prize*. [[online](#)]
 89. MS Dresselhaus. Optical properties of solids. *Solid State Phys – Part II*. MIT [[online](#)]
 90. Townes CH. The first laser. *A Century of Nature*. ©2003 Univ Chicago Press; 380. [[online](#)]
 91. Laser Diode. *Wikipedia*. [last reviewed 2023 Feb 14]. [[online](#)]
 92. Baldwin R. Oct. 9, 1962: First visible LED is demonstrated. *Wired*. 2012 Oct 9. [[online](#)]
 93. Home K, William N, Wehbeh C. LED inventor Nick Holonyak reflects on discovery 50 Years later. *GE Press Release*. 2012 Oct 9. [[online](#)]
 94. Mester E, Szende B, Gärtner P. The effect of laser beams on the growth of hair in mice. *Radiobiol Radiother (Berl)*. 1968; 9(5): 621-6. [[PubMed](#)]
 95. Mester E, Spiry T, Szende B, Tota JG. Effect of laser rays on wound healing. *Am J Surg*. 1971 Oct; 122(4): 532-535. [[PubMed](#)]
 96. Smith KC. Laser (and LED) therapy is phototherapy. *Photomed Laser Surg*. 2005 Feb; 23(1): 78-80. [[PubMed](#)][[online](#)]
 97. Anders JJ, Lanzafame RJ, Arany PR. Low-level light/laser therapy versus photobiomodulation therapy. *Photomed Laser Surg*. 2015 Apr; 33(4): 183-184. [[online](#)]
 98. Terminology. *North American Association for Photobiomodulation Therapy (NALT)*. [[online](#)]
 99. Schmidt MH, Bajic DM, Reichert KW, Martin TS, Meyer GA, Whelan HT. Light-emitting diodes as a light source for intra-operative photodynamic therapy. *Neurosurgery*. 1996; 38(3), 552-556. [[PubMed](#)][[online](#)]

100. Whelan HT, Houle JM, Donohoe DL, Bajic DM, Schmidt MH, Reichert KW, Weyenberg GT, Larson DL, Meyer GA, Caviness JA. Medical applications of space light-emitting diode technology-space station and beyond. *Space Tech App Int'l. Forum 1999*; 458: 3-15 [\[online\]](#)[\[online\]](#)
101. Whelan HT, Houle JM, Whelan NT, Donahue DL, Cwiklinski J., Schmidt MH, Gould L, Larson DL, Meyer GA, Cevenini V, Stinson H. The NASA light-emitting diode medical program – progress in space flight and terrestrial applications. *Space Tech App Int'l. Forum 2000*; 504: 37-43. [\[online\]](#) [\[online\]](#)
102. Heiskanen V, Hamblin MR. Photobiomodulation: Lasers vs. light emitting diodes? *Photochem Photobio Sci.* 2018 Aug 8; 17(8): 1003-1017 [\[PubMed\]](#)
103. Kim WK, Calderhead RG. Is light-emitting diode phototherapy (LED-LLLT) really effective? *Laser Ther.* 2011; 20(3): 205-215. [\[PubMed\]](#)
104. Shah HR, Yen MT. New LED phototherapy device for skin rejuvenation. *Ophthalmology Times.* 2008 Jun 1; 33(11). [\[online\]](#)
105. Williams RK, Lin KH. 3D bendable printed circuit board with redundant interconnections. *US patent no. US20170118838A1.* issued 2017 Apr 27. [\[online\]](#)
106. Williams RK. Advances in photobiomodulation therapy - a new paradigm in pain management. *J. Pain Relief.* 2017 Oct 19; 6(6). [\[online\]](#)
107. Williams RK, Lin KH, Schell D, Leahy JP. Phototherapy system with dynamic drive for light-emitting diodes. *US patent no. US20190373687A1 (divisional).* Issued 2019 Dec 5 [\[online\]](#)
108. Karu T. Is it time to consider photobiomodulation as a drug equivalent? *Photomed Laser Surg.* 2013 May; 31(5): 189-191 [\[PubMed\]](#)
109. Fitzpatrick R. Laws of geometric optics. *Univ Texas.* [last reviewed 2014 Jun 27]. [\[online\]](#)
110. Doctors using laser therapy to treat COVID-19 patients report positive outcomes. *Bit Flow.* 2020 Oct 1. [\[online\]](#)
111. Williams RK, Raimondo J, Cahn D, Williams A, Schell D. Whole-organ transdermal photobiomodulation (PBM) of COVID-19: A 50-patient case study. *J Biophotonics.* [first published 2021 Oct 17], 2022 Feb; 15(2) [\[PubMed\]](#)
112. Qian ET, Gatto CL, Amusina O, et al. Assessment of awake prone positioning in hospitalized adults with COVID-19. *JAMA.* 2020 Apr 18; 82(6): 612-621. [\[JAMA\]](#)
113. Su CT, Chiu FC, Ma SH, Wu JH. Optimization of photobiomodulation dose in biological tissue by adjusting the focal point of lens. *Photonics.* 2022 May, 9(5): 350 [\[online\]](#)
114. Mayerhöfer TG, Pahlow S, Popp J. The Bouguer-Beer-Lambert law: Shining light on the obscure. *Chem Europe.* [first published 2020 Jul 14]. 2020 Sep 15; 21 (18): 2029-2046 [\[online\]](#)
115. Han D, Xua J, Wanga Z, Yanga N, Lib X, Qian Y, Lib G, Daib R, Xu S. Penetrating effect of high-intensity infrared laser pulses through body tissue. *RSC Adv.* 2018 Sep 19; 8: 32344-32357 [\[online\]](#)
116. Finlayson L, Barnard IRM, McMillan L, Ibbotson SH, Brown CTA, Eadie E, Wood K. Depth penetration of light into skin as a function of wavelength from 200 to 1000 nm. *Photochem Photobio.* [first published 2021 Oct 26] 2022 Jul/Aug; 98(4): 971-984. [\[online\]](#)
117. Barnard IRM, Tierney P, Campbell CL, McMillan L, Moseley H, Eadie E, Brown CTA, Wood K. Quantifying direct DNA Damage in the basal layer of skin exposed to UV radiation from sunbeds. *Photochem Photobio.* 2018 May; 94(5). [\[online\]](#)
118. Chiappa F, Frascella B, Vigezzi GP, Moro M, Diamanti L, Gentile L, Lago P, Clementi N, Signorelli C, Mancini N, Odone A. The efficacy of ultraviolet light-emitting technology against coronaviruses: a systematic review. *J Hosp Infect.* [published 2021 May 21] 2021 Aug; 114: 63–78. [\[PubMed\]](#)
119. Rathnasinghe R, Jangra S, Miorin L, Schotsasert M, Yahnke C, García-Sastre A. The virucidal effects of 405 nm visible light on SARS-CoV-2 and influenza A virus. *Sci Rep.* 2021 Sep 1. [\[online\]](#)
120. Hamblin M, Demidova TN. Mechanisms of low level light therapy. *Proc SPIE.* 2006 Mar; 6140(614001): 1605-7422. [\[online\]](#)
121. Anderson PR, Parrish JA. The optics of human skin. *J invest Dermatol.* 1981 Jul; 77(1): 13-19. [\[online\]](#)
122. Marschall S, Pedersen C, Andersen PE. Investigation of the impact of water absorption on retinal OCT imaging in the 1060 nm range. *Biomed Optics Express.* 2012 Jul 1; 3(7): 1620-1631. [\[PubMed\]](#)
123. Hudson DE, Hudson DO, Winger JM, Richardson BD. Penetration of laser light at 808 and 980 nm in bovine tissue samples. *Photomed Laser Surgery.* 2013; 31(4): 163-168. [\[online\]](#)

124. Ash C, Dubec M, Donne K, Bashford T. Effect of wavelength and beam width on penetration in light-tissue interaction using computational methods. *Lasers Med Sci.* 2017; 32(8): 1909-1918. [[PubMed](#)]
125. Zhao HQ, Fairchild PW. Dependence of light transmission through human skin on incident beam diameter at different wavelengths. *Proc SPIE Laser-Tissue Interaction IX.* 1998 May 13; 3254. [[online](#)]
126. Stecco C, Sfriso MM, Porzionato A, Rambaldo A, Albertin G, Macchi V, de Caro R. Microscopic anatomy of the visceral fasciae. *J. Anat.* 2017 Mar 3; 231: 121-128. [[online](#)]
127. Bashkatov AN, Genina EA, Tuchin VV. Optical properties of skin, subcutaneous, and muscle tissues: A review. *J Innov Opt Health Sci.* 2011 Jan; 4(01): 9-38. [[online](#)]
128. Shimojo Y, Nishimura T, Hazama H, Ozawa T, Awazu K. Measurement of absorption and reduced scattering coefficients in Asian human epidermis, dermis, and subcutaneous fat tissues in the 400- to 1100-nm wavelength range for optical penetration depth and energy deposition analysis. *J Biomed Opt.* 2020 Apr; 25(4): 045002. [[PubMed](#)]
129. Lister T, Wright PA, Chappell PH. Optical properties of human skin. *J Biomed Optics.* 2012 Sep 24; 17(9): 090901. [[online](#)]
130. Koster PM. Near infrared light penetration in human tissue: An analysis of tissue structure and heterogeneities. *Masters Thesis, Marquette Univ.* 2022 Dec; 739. [[online](#)]
131. Understanding penetration depth vs. wavelength for biosensor applications. *Maxim Integrated App Note 6433.* [[online](#)]
132. Hong Duyen TTH, TA. Simulating low-level laser propagation from skin surface to lumbar disc, knee, femur and prostate gland by Monte Carlo method. *American Academic Scientific Research Journal for Engineering, Technology, and Science.* 2020 Apr 8; 67(1): 17-24 [[online](#)]
133. Arslan H. simulation study for the penetration depth of red and near infrared light in muscle tissue. *4th Intl Symp Innov Tech Eng Sci (ISITES 2016).* 2016 Nov 3-5; 329-333 [[online](#)]
134. Stolik S, Delgado Atencio JAD, Pérez AM, Lorenzo A. Measurement of the penetration depths of red and near infrared light in human “ex vivo” tissues. *J Photochem Photobio. B, Biology.* 2000 Oct; 57(2-3): 90-93. [[online](#)]
135. Jagdeo J, Adams LE, Brody NI, Daniel B, Siegel DM. Transcranial red and near infrared light transmission in a cadaveric model. *PLoS One.* 2012 Oct; 7(10): e47460. [[online](#)]
136. Skin penetration time-profiles for continuous 810 nm and superpulsed 904 nm lasers in a rat model. 2007 Feb; *Acupunct Electrother Res.* 32(1-2): 81-86. [[PubMed](#)]
137. Ozgulbas D. NIR light transmission through skin and muscle. *Thesis – Biomed Eng Bioeng Commons at NJIT.* 2013 May; 164. [[online](#)]
138. Pitzschke A, Seydoux L, et al. Red and NIR light dosimetry in the human deep brain. *Phys Med Bio.* 2015 Mar; 60(7): 2921-2937. [[PubMed](#)]
139. Tedford CE, DeLapp S, Jacques S, Anders J. Quantitative analysis of transcranial and intraparenchymal light penetration in human cadaver brain tissue. *Lasers Surg Med.* 2015 Apr; 47(4): 312-322. [[PubMed](#)]
140. Pitzschke A, Lovisa B, Seydoux O, Zellweger M, Pfeleiderer M, Haenggi M, Oertel M, Tardy Y, G. Wagnières G. Optical properties of the deep brain in the red and NIR: changes observed under in-vivo, post-mortem, frozen and formalin-fixated conditions. *Med Laser Apps Laser-Tissue Interact – VII SPIE Proceedings* [© 2015 Optica Publishing Group] 2015; 954207. [[online](#)]
141. Cassano P, Tran AP, Katnani H, Bleier BS, Hamblin MR, Yuan Y, Fang Q. Selective photobiomodulation for emotion regulation: model-based dosimetry study. *Neurophotonics.* 2019 Feb; 6(1): 015004. [[online](#)]
142. Catanzaro B, Streeter J, De Taboada L. Review of technology development and clinical trials of transcranial laser therapy for acute ischemic stroke treatment. *2010 Proc SPIE – Intl Soc Opt Eng.* 2010 Feb; 7552: 10 [[online](#)]
143. Peixoto dos Santos JGR, Zaninotto ALC, Zângaro RA, Carneiro AMC, Neville LS, Ferreira de Andrade A, Teixeira MJ, Paiva WS. Effects of transcranial LED therapy on the cognitive rehabilitation for diffuse axonal injury due to severe acute traumatic brain injury: study protocol for a randomized controlled trial. 2018 Ape 24; 19(249). [[online](#)]
144. Jara C, Buendía D, Ardiles A, Muñoz P, Tapia-Rojas C. Transcranial red LED therapy: A promising non-invasive treatment to prevent age-related hippocampal memory impairment. Chapter 8 of *Hippocampus - Cytoarchitecture and Diseases.* [© Intech Open Ltd] 2021 Oct 25. [[online](#)]
145. Henderson TA, Morries LD. Near-infrared photonic energy penetration: can infrared phototherapy effectively reach the human brain? *Neuropsychiatric Disease Treatment.* 2015 Aug 21: 2191-2208. [[online](#)]

146. Hamblin MR. Shining light on the head: Photobiomodulation for brain disorders. *BBA Clinical*. 2016 Dec; 6: 113-124. [\[online\]](#)
147. Saucedo CL, Courtois EC, Wade ZS, Kelley MN, Kheradbin N, Barrett DW, Gonzalez-Lima F. Transcranial laser stimulation: Mitochondrial and cerebrovascular effects in younger and older healthy adults. *Brain Stim*. 2021 Mar-Apr; 14(2); 440-449. [\[online\]](#)
148. Yuan Y, Cassano P, Pias M, Fang Q. Transcranial photobiomodulation with near-infrared light from childhood to elderliness: simulation of dosimetry. *Neurophotonics*. 2020 Feb 24; 7(1): 015009. [\[online\]](#)
149. Park JH, Kim DY, Schubert EF, Cho J, Kim JK. Fundamental limitations of wide-bandgap semiconductors for light-emitting diodes. *ACE Energy Lett*. 2018 Feb 13; 3: 655-662. [\[online\]](#)
150. McCauley L. Laser as a therapeutic modality. *VMX Vet Mtg Expo: 2013 Proc. (NAVC Conf 2013 Small Animal Exotics Proc)*. 2013. [\[online\]](#)
151. Clement M, Daniel G, Trelles M. Optimising the design of a broad-band light source for the treatment of skin. *J Cosmet Laser Ther*. 2005 Dec; 7(3): 177-89. [\[PubMed\]](#)
152. Song S, Kobayashi Y, Fujie MG. Monte Carlo simulation of light propagation considering characteristic of near-infrared LED and evaluation on tissue phantom. *Proc CIRP*. 2013; 5: 25-30. [\[online\]](#)
153. Heiskanen V, Hamblin MR. Photobiomodulation: Lasers vs. light emitting diodes? *Photochem Photobiol Sci*. 2018 Jul; 17: 1003-1017. [\[PubMed\]](#)
154. Chen X, Olga Korotkova O. Optical beam propagation in soft anisotropic biological tissues. *OSA Continuum* 2018 Nov 13; 1(3): 1055-1067 [\[online\]](#)
155. Laakso L, Richardson C, Cramond T. Quality of light - is laser necessary for effective photobiostimulation? *Aus Physio*. 1993; 39(2): 87-92. [\[PubMed\]](#)
156. Zalevsky Z, Belkin M. Coherence of light and generation of speckle patterns in photobiology and photomedicine. *Proc SPIE Mechanisms for Low-Light Therapy VII*. 2012; 8211: 82110J-1. [\[online\]](#)
157. Carp SA, Tamborini D, Mazumder D, Wu K-C, Robinson MB, Stephens KA, Shatrovov O, Lue N, Ozana N, Blackwell MH, Franceschini MA. Diffuse correlation spectroscopy measurements of blood flow using 1064 nm light. *J Biomed Opt*. 2020 Sep; 25(9): 097003-1. [\[online\]](#)
158. Karu T. Action spectra – Their importance for low level light therapy. *Photobiology.info* 2008 Oct 14: 1-30. [\[online\]](#)
159. Karu T. Primary and secondary mechanisms of action of visible to near-IR radiation on cells. *J Photochem Photobiology B: Bio*. 1999 Mar; 49(1): 1-17. [\[online\]](#)
160. Karu T, Kolyakov SF. Exact action spectra for cellular responses relevant to phototherapy. *Photomed Laser Surg*. 2005 Sep; 23(4): 355-361. [\[online\]](#)
161. Re-evaluation of the near infrared spectra of mitochondrial cytochrome c oxidase: Implications for non invasive in vivo monitoring of tissues. *Biochimica Biophys Acta Bioenerg*. 2014 Nov; 1837(11): 1882–1891. [\[PubMed\]](#)
162. Hashmi JT, Huang YY, Sharma SK, Kurup DB, De Taboada L, Carroll JD, Hamblin MR. Effect of pulsing in low-level light therapy. *Lasers Surg Med*. 2010 Aug; 42(6): 450–466. [\[PubMed\]](#)
163. Kim HB, Baik KY, Chung PH, Chung JH. Pulse frequency dependency of photobiomodulation on the bioenergetic functions of human dental pulp stem cells. *Sci Rep*. 2017 Nov 21; 7(15927). [\[online\]](#)
164. Barбора A, Bohar O, Sivan AA, Magory E, Nause A, Minnes R. Higher pulse frequency of near-infrared laser irradiation increases penetration depth for novel biomedical applications. *PLoS One*. 2021 Jan 7; 16(1): e0245350. [\[online\]](#)
165. Keshri GK, Gupta A, Yadav A, Sharma SK, Singh SB. Photobiomodulation with pulsed and continuous wave near-infrared laser (810 nm, Al-Ga-As) augments dermal wound healing in immunosuppressed rats. *PLoS One*. 2016 Nov 18; 11(11): e0166705. [\[PubMed\]](#)
166. Chen Z, Zhang R, Qin H, Jiang H, Wang A, Zhang X, Huang S, Sun M, Fan X, Lu Z, Li Y, Liu S, Liu M. The pulse light mode enhances the effect of photobiomodulation on B16F10 melanoma cells through autophagy pathway. *Lasers Med Sci*, 2023 Feb 15; 38(1): 71. [\[online\]](#)
167. Ueda Y, Shimizu N. Effects of Pulse Frequency of Low-Level Laser Therapy (LLLT) on Bone Nodule Formation in Rat Calvarial Cells. *J Clinical Laser Med Surg*. 2003 Nov; 21(5): 271-277. [\[online\]](#)
168. Ilic S, Leichter S, Streeter J, De Taboada L, Oron U. Effects of power densities, continuous and pulse frequencies, and number of sessions of low-level laser therapy on intact rat brain. *Photomed Laser Surg*. 2006 Sep; 24(4): 458-466. [\[online\]](#)

169. Zecha J, Raber-Durlacher JE, Nair RG, Epstein JB, Elad S, Hamblin MR, Barasch A, et al. Low-level laser therapy/photobiomodulation in the management of side effects of chemoradiation therapy in head and neck cancer: part 2: proposed applications and treatment protocols. *Supportive Care in Cancer*. 2016 Mar; 24(6): 2793–2805. [online]
170. Lapchak PA, Salgado KF, Chao CH, Zivin JA. Transcranial near-infrared light therapy improves motor function following embolic strokes in rabbits: An extended therapeutic window study using continuous and pulse frequency delivery modes. *Neuroscience*. 2007 Sep; 148(4): 907-914. [online]
171. Kaub L, Schmitz C. More than ninety percent of the light energy emitted by near-infrared laser therapy devices used to treat musculoskeletal disorders is absorbed within the first ten millimeters of biological tissue. *Biomedicines*. 2022 Dec 9; 10(12): 3204. [PubMed]
172. Barbora A, Bohar O, Ariel Alexander Sivan AA, Magory E, Nause A, Minnes R. Higher pulse frequency of near-infrared laser irradiation increases penetration depth for novel biomedical applications. *PLoS ONE* 16(1): e0245350. [online]
173. Williams RK. Into to Photobiomodulation (PBM): Cytology, physiology & therapeutics. *Five Branches University (lecture excerpts)* 2020 Feb 1: 1-99. [available by request]
174. Ruggiero E, De Castro SA, Habtemariam A, Salassa L. Upconverting nanoparticles for the near infrared photoactivation of transition metal complexes: new opportunities and challenges in medicinal inorganic photochemistry. *Dalton Trans*. 2016 Aug; 45(33): 1302-13020. [online]
175. Zein R, Selting W, Michael R, Hamblin MR. Review of light parameters and photobiomodulation efficacy: dive into complexity. *J Biomed Opt*. 2018 Dec 11; 23(12): 120901 [PubMed]
176. Al-Ghamdi KM, Kumar A, Moussa NA. Low-level laser therapy: a useful technique for enhancing the proliferation of various cultured cells. *Lasers Med Sci*. 2012 Jan; 27(1): 237-249 [PubMed]
177. Rola P, Włodarczyk S, Lesiak M, Doroszko A, Włodarczyk A. Changes in cell biology under the influence of low-level laser therapy. *Photonics* 2022 Jul 20; 9(7): 502. [online]
178. Hamblin MR, Ferraresi C; Huang YY; De Freitas LF; Carroll JD. Introduction. *Low-Level Light Therapy: Photobiomodulation*. [© 2018 SPIE Press Books] 2018 Jan 20: 1-388. [online]
179. Sommer AP, Pinheiro ALB, Mester A, Franke R-P, Whelan A. Biostimulatory windows in low-intensity laser activation: lasers, scanners, and NASA's light-emitting diode array system. *J Clinical Laser Med Surg*. 2001 Mar; 19(1): 29-33. [online]
180. Huang YY, Sharma SK, Hamblin MR. biphasic dose response in low level light therapy – An update. *Dose Response*. 2011 Sep 2; 9(4): 602–618. [PubMed]
181. Liebert A, Capon W, Pang V, Vila D, Bicknell B, McLachlan C, Kiat H. Photophysical mechanisms of photobiomodulation therapy as precision medicine. *Biomed* 2023 Feb; 11(2): 237. [PubMed]
182. Kučera O, Cifra M. Cell-to-cell signaling through light: just a ghost of chance? *Cell Comm Signal*. 2013, 11(87). [PubMed]
183. Poyton RO, Ball KA. Therapeutic photobiomodulation: Nitric oxide and a novel function of mitochondrial cytochrome c oxidase. *Discovery Med*. 2011 Feb 20. [online]
184. Karu TI. Multiple roles of cytochrome c oxidase in mammalian cells under action of red and IR-A radiation. *IUBMB Life*. [first published 2010 Jul 28] 2010 Aug; 62(8): 607–610. [PubMed]
185. Barolet AC, Litvinov LV, Barolet D. Light-induced nitric oxide release in the skin beyond UVA and blue light: Red & near-infrared wavelengths. *Nitric Oxide*. 2021 Dec 1; 117: 16-25. [online]
186. Abate C, Luk D, Curran T. Transcriptional regulation by Fos and Jun in vitro: interaction among multiple activator and regulatory domains. *Mol Cell Bio*. 1991 Jul; 11(7): 3624-3632. [PubMed]
187. Sommer AP, Schemmer P, Pavláth AE, Försterling H-D, Mester AR, Trelles MA. Quantum biology in low level light therapy: death of a dogma. *Annals Transl Med*. 2020; 8(7): 440. [online]
188. Pevna V, Horvath D, Wagnieres G, Huntosova V. Photobiomodulation and photodynamic therapy-induced switching of autophagy and apoptosis in human dermal fibroblasts. *J. Photochem Photobio B: Biology*. 2012 Sep; 234(112539). [online]
189. Fink SL, Cookson BT. Apoptosis, pyroptosis, and necrosis: mechanistic description of dead and dying eukaryotic cells. *Infect Immun*. 2005 Apr; 73(4): 1907–1916. [PubMed]
190. Raker V, Becker C, Steinbrink K. The cAMP pathway as therapeutic target in autoimmune

- and inflammatory diseases. *Front. Immunol.* 2016 Mar 31; 7(123). [online]
191. Cardoso FdS, Mansur FCB, Lopes-Martins RAB, Gonzalez-Lima F, Gomes da Silva S. Transcranial laser photobiomodulation improves intracellular signaling linked to cell survival, memory and glucose metabolism in the aged brain: a preliminary study. *Front Cell Neurosci.* 2021 Sep 3; 15. [online]
 192. Pan LC, Hang NLT, Colley MMS 1, Chang J, Hsiao YC, Lu LS, Li BS, Chan CJ, Yang TS. Single cell effects of photobiomodulation on mitochondrial membrane potential and reactive oxygen species production in human adipose mesenchymal stem cells. *Cells* 2022 Mar 11; 11(6): 972 [online]
 193. Jonckheere AI, Smeitink JAM, Rodenburg RJT. Mitochondrial ATP synthase: architecture, function and pathology. *J Inherit Metab Dis.* 2012; 35(2): 211–225. [PubMed]
 194. You M, Chen L, Zhang D, Zhao P, Chen Z, Qin EQ, Gao Y, Davis MM, Yang P. Single-cell epigenomic landscape of peripheral immune cells reveals establishment of trained immunity in individuals convalescing from COVID-19. *Nat Cell Biol.* 2021 Jun; 23(6): 620-630. [PubMed]
 195. Wang Y, Huang YY, Wang Y, Lyu P, Hamblin MR. Red (660 nm) or near-infrared (810 nm) photobiomodulation stimulates, while blue (415 nm), green (540 nm) light inhibits proliferation in human adipose-derived stem cells. *Sci Reports.* 2017 Aug 10; 7(7781). [online]
 196. Yang X, Ha G, Needleman DJ. A coarse-grained NADH redox model enables inference of subcellular metabolic fluxes from fluorescence lifetime imaging. *Biochem Chem Bio Phys Living Sys* 2021 Nov 22; 10(e73808): 1-44. [online]
 197. Hamblin MR. Mechanisms and mitochondrial redox signaling in photobiomodulation. *Photochem Photobiol.* 2018 Mar; 94(2): 199-212. [PubMed]
 198. 670 nm photobiomodulation improves the mitochondrial redox state of diabetic wounds. *Quant Imaging Med Surg.* 2021 Jan; 11(1): 107-118. [PubMed]
 199. Pfeilschifter J, Eberhardt W, Beck KF. Regulation of gene expression by nitric oxide. *Pflügers Archiv - Euro J Phys.* 2001 Jul; 442(4): 479-486. [online]
 200. Kim YM, Son K, Hong SJ, Green A, Chen JJ, Tzeng E, Hierholzer C, Billiar TR. Inhibition of protein synthesis by nitric oxide correlates with cytostatic activity: nitric oxide induces phosphorylation of initiation factor eIF-2 α . *Molec Med.* 1998 Mar 1; 4: 179–190. [online]
 201. Zenz R, Eferl R, Scheinecker C, Redlich K, Smolen J, Schonhaller HB, Kenner L, Tschachler E, Wagner EF. Activator protein 1 (Fos/Jun) functions in inflammatory bone and skin disease. *Arthritis Res Ther* 2008 Jan 18. 10(201). [online]
 202. Dompe C, Moncrieff L, Matys J, et al. Photobiomodulation – Underlying mechanism and clinical applications. *J Clin Med.* 2020 Jun; 9(6): 1724. [PubMed]
 203. Walski T, Dabrowska K, Drohomirecka A, Zuk N, Trochanowska-Pauk N, Witkiewicz W, Komorowska M. The effect of red-to-near-infrared (R/NIR) irradiation on inflammatory processes. *Int J Rad Bio.* 2019 Jun. [online]
 204. Kitchen JC, Berman M, Halper J, Chazot P. Rationale for 1068 nm photobiomodulation therapy (PBMT) as a novel, non-invasive treatment for COVID-19 and other coronaviruses: roles of NO and Hsp70. *Int. J. Mol. Sci.* 2022, 23(9); 5221. [online]
 205. Opal SM, DePalo VA. Anti-inflammatory cytokines. *Chest.* 2000 Apr; 117(4): 1162-1172. [PubMed]
 206. Wen AY, Kathleen, Sakamoto M, Mille LS. The role of the transcription factor CREB in immune function. *J Immunol.* 2010 Dec 1; 185(11): 6413–6419. [PubMed]
 207. Don J, Stelzer G. The expanding family of CREB/CREM transcription factors that are involved with spermatogenesis. *Mol Cell Endocrinol.* 2002 Feb 22; 187(1-2): 115-124. [PubMed]
 208. Bhavya BC, Haridas M. Anti-inflammatory molecules: Immune system mediators. *Bioresources Bioprocess Biotech.* [© 2017 Springer, Singapore] 2017; 235-268. [online]
 209. Parmet S. Boosting the anti-inflammatory action of the immune system. *UIC Today.* 2003 Mar 28. [online]
 210. Colombo E, Signore A, Aicardi S, Zekiy A, Utyuzh A, Benedicenti S, Andrea Amaroli A. Experimental and clinical applications of red and near-infrared photobiomodulation on endothelial dysfunction: a review. *Biomedicines* 2021 Mar 9; 9(3): 274. [online]
 211. Elblbesy MA. Comparative in vitro study: examining 635 nm laser and 265 nm ultraviolet interaction with blood. *Photobio Photomed Laser Surg.* 2019 Jun 7; 37(6). [PubMed]
 212. Buzinari TC, De Moraes TF, Cárnio EC, Lopes LA, Salgado HC, Rodrigues GJ. Photobiomodulation induces hypotensive

- effect in spontaneously hypertensive rats. *Lasers Med Sci.* 2020 Apr; 35(3): 567-572. [[PubMed](#)]
213. Walski T, Grzeszczuk-Kuć K, Gałęcka K, Trochanowska-Pauk N, Bohara R, Czernski A, Szuldrzyński K, Królikowski W, Detyna J, Komorowska M. Near-infrared photobiomodulation of blood reversibly inhibits platelet reactivity and reduces hemolysis. *Sci Rep.* 2022 Mar 8; 12(4042). [[online](#)]
214. Cheng-Yi Liu TCY, Cheng L, Su WJ, Zhang YW, Shi Y, Liu AH, Zhang LL, Qian ZY. Randomized, double-blind, and placebo-controlled clinic report of intranasal low-intensity laser therapy on vascular diseases. *Int J Photoenergy.* 2012 Mar 27; 2012(489713): 5. [[online](#)]
215. Hughes MP, Kruchek EJ, Beale AD, Kitcatt SJ, Qureshi S, Trott ZP, Charbonnel O, Paul A, Agbaje PA, Erin A, Henslee EA, Dorey DA, Lewis R, Labeed FH. V_m-related extracellular potentials observed in red blood cells. *Sci Rep.* 2021 Sep 30; 11(19446). [[online](#)]
216. Komorowska M, Cuissot A, Czarnołęski A, Białas W. Erythrocyte response to near-infrared radiation. *J. Photochem Photobio B: Biology.* 2002 Nov; 68(2-3): 93-100. [[online](#)]
217. Chen XY, Huang YX, Liu WJ, Yuan ZJ. Membrane surface charge and morphological and mechanical properties of young and old erythrocytes. *Current Appl Phys.* 2007 Apr; 7(1): e94-e96. [[online](#)]
218. Walski T, Grzeszczuk-Kuć K, Berlik W, Synal-Kulczak I, Bohara R, Detyna J, Komorowska M. Effect of near-infrared blood photobiomodulation on red blood cell damage from the extracorporeal circuit during hemodialysis in vitro. *Photonics.* 2022 May 14; 9(5), 341 [[online](#)]
219. Walski T, Drohomirecka A, Bujok J, Czernski A, Wąz G, Trochanowska-Pauk N, Gorczykowski M, Romuald Cichoń R, Komorowska M. Low-Level light therapy protects red blood cells against oxidative stress and hemolysis during extracorporeal circulation. *Front Physiol.* 2018 May 31; 9. [[online](#)]
220. Salehpour F, Khademi M, Bragin DE, DiDuro JO. Photobiomodulation therapy and the lymphatic system: promising applications for augmenting the brain lymphatic drainage system. *Int J Mol Sci.* 2022 Mar; 23(6): 2975. [[PubMed](#)]
221. Cios A, Ciepielak M, Szymanski L, Lewicka A, Cierniak S, Stankiewicz W, Mendrycka M, Sławomir Lewicki S. Effect of different wavelengths of laser irradiation on the skin cells. *Int J Mol Sci* 2021 Feb 19; 22(5): 2437. [[online](#)]
222. Urquhart EL, Wanniarachchi H, Wang X, Gonzalez-Lima F, Alexandrakis G, Liu H. Transcranial photobiomodulation-induced changes in human brain functional connectivity and network metrics mapped by whole-head functional near-infrared spectroscopy in vivo. *Biomedical Optics Express* 2020 Oct; 11(10): 5783. [[online](#)]
223. Long COVID or post-COVID conditions. CDC – Center Disease Cont Prev. [last reviewed 2022 Dec 16] [[online](#)]
224. Chippa V; Aleem A; Anjum F. Post acute coronavirus (COVID-19) syndrome. StatPearls [Internet]. [© 2023 Treasure Island (FL): StatPearls Publishing] [last reviewed 2023 Feb 3] [[PubMed](#)]
225. Kanne JP, Little BP, Schulte JL, Haramati A, Haramati LB. Long-term lung abnormalities associated with COVID-19 pneumonia. *Radiology.* 2022 Aug 30; 306(2). [[online](#)]
226. Wang C, Yu C, Jing H, Wu X, Novakovic VA, Xie R, Shi J. Long COVID: The nature of thrombotic sequelae determines the necessity of early anticoagulation. *Front Cell Infect Microbio.* 2022 Apr 5; 12 [[online](#)]
227. Cardiac arrhythmias in post-COVID syndrome: Prevalence, pathology, diagnosis, and treatment. *Viruses.* 2023 Jan 29, 15(2), 389. [[online](#)]
228. Rohun J, Dorniak K, Faran A, Kochańska A, Zacharek D, Daniłowicz-Szymanowicz L. Long COVID-19 myocarditis and various heart failure presentations: A case series. *J Cardiovasc Dev Dis.* 2022 Dec; 9(12): 427. [[PubMed](#)]
229. Kunkalikal B. Heart symptoms persist in 10% of patients with long-COVID. *News-Medical.* 2023 Jan 23. [[online](#)]
230. Ackerman T. Reduced myocardial blood flow new clue in COVID-19's effect on the heart. *Houston Methodist.* 2022 Oct 11. [[online](#)]
231. Bogariu AM, Dumitrascu DL. Digestive involvement in the long-COVID syndrome. *Med Pharm Rep.* 2022 Jan; 95(1): 5–10. [[PubMed](#)]
232. Lamb LE, Timar R, Wills M, Dhar S, Lucas SM, Komnenov D, Chancellor, MB Nivedita Dhar N. Long COVID and COVID-19-associated cystitis (CAC). *Int Urol Nephrol.* 2022; 54(1): 17–21. [[PubMed](#)]
233. Falkenhain-López D, Agud-Dios M, Ortiz-Romero PL, Sánchez-Velázquez A. COVID-19-related acute genital ulcers. *J Eur Acad*

- Dermatol Venereol.* 2020 Nov; 34(11): e655–e656. [PubMed]
234. Selek A, Güçlü M, Bolu SE. COVID-19 pandemic: what about the gonads? *Hormones (Athens)*. 2021; 20(2): 259–268. [PubMed]
235. Sutherland S. Long COVID now looks like a neurological disease, helping doctors to focus treatments. *Sci Amer.* 2023 Mar 1. [online]
236. Houben-Wilke S, Goertz YMJ, Delbressine JM, Roy Meys R, Machado FVC, Van Herck M, Vaes AW, Franssen FME, Vijlbrief H, Burtin C, Posthuma R, Janssen DJA, Spies Y, Van 't Hul AJ, Spruit MA. The Impact of Long COVID-19 on Mental Health: Observational 6-Month Follow-Up Study. *JMIR Ment Health.* 2022 Feb; 9(2): e33704. [PubMed]
237. Lemogne C, Gouraud C, Pitron V, Brigitte Ranquee B. Why the hypothesis of psychological mechanisms in long COVID is worth considering. *J Psychosom Res.* 2023 Feb; 165: 111135. [PubMed]
238. Guo YR, Cao QD, Hong ZS, Tan YY, Chen SD, Jin HJ, Tan KS, Wang DY, Yan Y. The origin, transmission and clinical therapies on coronavirus disease 2019 (COVID-19) outbreak – an update on the status. *Mil Med Res.* 2020; 7: 11. [PubMed]
239. Williams RK, Lin K. Photobiomodulation for health maintenance. *Applied BioPhotonics Newsletter COVID-19 Update.* 2020 Mar 14 [available upon request].
240. Cleverley J, Piper J, Jones MM. The role of chest radiography in confirming covid-19 pneumonia. *BMJ* 2020; 370. [online]
241. Ken L, Hung TC, Wu TH. LightDr™ case study of whole organ transcutaneous photobiomodulation (PBM) on COVID-19 – An empirical case study in Taiwan. 2022 *International Paramedic Summit and AI Artificial Intel Med App Acad Forum.* Taipei 2022 May.
242. Masic I, Miokovic M, Muhamedagic B. Evidence Based Medicine – New Approaches and Challenges. *Acta Inform Med.* 2008 Dec; 16(4): 219–225. [PubMed]
243. Lim L, Hosseinkhah N, Buskirk MV, Berk A, et al. Home-use photobiomodulation device treatment outcomes for COVID-19. *MedRxiv Preprint.* 2022 Jun 17. [online]
244. Vetrici MA, Mokmeli S, Bohm AR, Monici M, Sigman SA. Evaluation of adjunctive photobiomodulation (PBMT) for COVID-19 pneumonia via clinical status and pulmonary severity indices in a preliminary trial. *J Inflamm Res.* 2021; 14: 965–979. [PubMed]
245. De Marchi T, Frâncio F, Ferlito JV, Weigert R, de Oliveira C, Merlo AP, Pandini DL, Pasqual-Júnior BA, Giovanella D, Tomazoni SS, Leal-Junior EC. Effects of photobiomodulation therapy combined with static magnetic field in severe COVID-19 patients requiring intubation: a pragmatic randomized placebo-controlled trial. *J Inflamm Res.* 2021 Jul 24; 2021(14): 3569-3585. [online]